THERMAL AND PHOTODEHYDROGENATION REACTIONS OF TERPENES OVER ZEOLITES

By

Esra TUZCUOĞLU

A Dissertation Submitted to the
Graduate School in Partial Fulfillment of the
Requirements for the Degree of

MASTER OF SCIENCE

Department: Chemistry

İzmir Institute of Technology
İzmir, Turkey

September, 2003

ACKNOWLEDGEMENTS

I would like to thank to Prof. Dr. Levent Artok and Prof. Dr.Sıddık İçli for their supervision, help, support and encouragement during this thesis.

I would like to thank to Prof. Dr. Devrim Balköse for supplying synthesized amorphous silica.

I would like to thank to my Institution, İzmir Institute of Technology, for providing full time Research Assistantship and the Research Funding Office of İzmir Institute of Technology for financial support during my graduate study. Special thanks to all research assistants, especially to my colleagues Ms. Müge Açıkel and Mrs. Hatice Bulut for their friendship and their helps during this thesis.

Finally, I would like to thank to my family, for their help, support, patience and love.

ABSTRACT

In this thesis study, catalytic activity of cation exchanged (Na^+, Li^+, Ca^{2+}, K^+, Cs^+) zeolite Y, especially NaY, and various microporous and mesoporous (Na exchanged, Beta, Mordenite, and NaX, CsNaX, MCM-41, Montmorillonite KSF and amorphous Silica) catalysts was investigated in the dehydrogenation reaction of terpenes to p-cymene.

The results suggested that, there are two types of acid sites are present in cation exchanged zeolites from NH_4Y, which are Brønsted and Lewis sites. α-terpinene, disproportionated by Brønsted acid catalysis into 3-p-menthene and p-cymene, and p-cymene was also formed by direct dehydrogenation of α-terpinene can possibly occur with the participation of Lewis acid sites in cation exchanged zeolite Y. Best conversion to p-cymene were observed in the NaHY, LiHY and CaHY exchange from NH_4Y that have relatively small cations, which more acidic than the larger ones.

With the catalysts that have Brønsted acid sites except ion-exchanged zeolite Y, no conversion or only acid catalyzed isomerization reactions occur that shows the Brønsted acidity was not enough to catalyze the dehydrogenation of α-terpinene. Also Lewis acidic character and the structure morphology are the most important factors affecting the conversion. Lewis acidity is influenced from the cation and zeolite type.

ÖZ

Bu çalışmada, terpenelerin p-simen'e dehidrojenasyon reaksiyonlarında, katyon değişimine uğramış (Na^+, Li^+, Ca^{2+}, K^+, Cs^+) zeolit Y, özellikle NaY, çeşitli mikro ve mezogözenekli (Na ile katyon değiştirmiş Beta ve Mordenit, NaX, CsNaX, MCM-41, Montmorillonit KSF ve amorphous Silica) katolizörlerin katalitik aktiviteleri incelenmiştir.

Sonuçlar, katyon değişimine uğramış NH_4Y' nin Brønsted ve Lewis olmak üzere iki tip asidik kısma sahip olduğunu göstermiştir. α-terpinen Bronsted asit kataliziyle 3-p-mentin ve p-simen'e dönüşmek üzere disproporsiyona uğramıştır. Ayrıca, α-terpinen'in direkt dehidrojenasyonu ile oluşmuş p-simen, katyon değiştirmiş zeolit Y içinde Lewis asit kısımlarının katkısıyla oluşabilmektedir. Asidik özelliği fazla olan göreceli olarak daha küçük katyonlara sahip NH_4Y' den katyon değişimi ile elde edilen NaHY, LiHY ve CaHY içinde en iyi p-simen oluşumu gözlenmiştir.

İyon değiştirmiş zeolit Y hariç Brønsted asit kısımlarına sahip katalizörler ile dönüşüm gözlenememiş yada sadece asit katalizli izomerizasyon reaksiyonları meydana gelmiştir. Bu, Bronsted asitliğinin α-terpinen'in dehidrojenasyonunu katalizlemek için yeterli olmadığını göstermektedir. Ayrıca Lewis asidik karakteri ve morfolojik yapısı dönüşümü etkileyen en önemli etmenlerdendir. Lewis asitliği katyon ve zeolit tipinden etkilenmektedir.

TABLE OF CONTENTS

Page

LIST OF FIGURES viii
LIST OF TABLES x
CHAPTER 1. INTRODUCTION 1
CHAPTER 2. CATALYSIS 5
BACKROUND: CATALYSIS AND ZEOLITE CHEMISTRY 5
2.1. INTRODUCTION 5
2.2. ZEOLITES AS HETEREGENOUS CATALYSTS 6
2.3. ZEOLITES 7
2.4. STRUCTURAL FEATURES OF ZEOLITES 8
2.4.1. Zeolite Framework Structure 8
2.5. ZEOLITE PROPERTIES 9
2.5.1. Pore Structure And Molecular Sieving 9
2.5.2. Acidic And Basic Character Of Zeolite 12
2.5.3. Shape Selectivity 14
2.5.4. Ion Exchange 16
2.5.5. Ship-In-A-Bottle Sythesis 18
CHAPTER 3 INTRAZEOLITE DEHYDROGENATION OF TERPENES TO p-CYMENE 19
3.1. TERPENES 19
3.2. DEHYDROGENATION OF TERPENES TO p-CYMENE 21
3.2.1. Industrial Importance of p-Cymene 21
3.2.2. Production of p-Cymene 22
CHAPTER 4 EXPERIMENTAL STUDY 25
4.1. PREPARATION OF CATION EXCHANGED ZEOLITES 25
4.1.1. Preparation of NaHY 25
4.1.2. Preparation of LiHY, KHY and CaHY 25
4.1.3. Preparation of CsNaY 25
4.1.4. Preparation of CsNaX 26
4.1.5. Preparation of LiNaHY, CaNaHY and KnaHY 26

4.1.6. Preparation of HY 26
4.1.7. Preparation of calcined NaHY and NaY 26
4.1.8. Preparation of NaHβ and NaHMOR 26
4.1.9. Preparation of Perylene Loaded NaHY 27
4.1.9.1. UV-Visible Spectroscopy Analysis 28
4.1.10. Preparation of Pyridine Neutralized NaY 29
4.1.11. Preparation of Na_2CO_3 neutralized NaY 29
4.2. INTRAZEOLITE REACTIONS 29
4.2.1. Dehydrogenation Reactions 29
4.2.2. Photodehydrogenation and Photooxidation Reactions 31
4.2.3. Homogeneous Photooxidation Reactions 32
4.3. GC METHOD 32
4.3.1. Calculation of Reactant and Product Amount on GC 35
CHAPTER 5 RESULTS AND DISCUSSION 36
5.1. DEYHDROGENATIN REACTIONS OF α-TERPINENE WITHIN ZEOLITES 36
5.1.1. Effect of Catalyst and Cation Type 37
5.1.2. Effect of Effect of Drying 46
5.1.3. Effect of Reactant Amount 47
5.1.4. Effect of the Monoterpene Type 48
5.1.5. Effect of Irradiation and Sensitizer 48
5.1.6. Effect of the Acidic Properties of the NaY 49
5.2. X-RAY DIFFRACTION ANALYSIS 51
5.1.6. X-Ray Diffraction Analysis of NaY, NaHY and NH_4Y 51
5.1.6. X-Ray Diffraction Analysis Of Dried, Non-Dried And Calcined NaHY 52
CHAPTER 6 CONCLUSION 53
REFERENCES 54

LIST OF FIGURES

Figure 2.1. Silica and Alumina Tetrahedra 8

Figure 2.2. Pore size distribution in some adsorbents. (a) Dehydrated zeolite; (b) silica gel; (c) activated carbon 9

Figure 2.3. Pore topology of some common zeolites 10

Figure.2.4. a) 12-Membered Ring Window and b) Cation Locations in Faujasite-type Zeolites 11

Figure 2.5. Formation of Brønsted Acid Sites 13

Figure 2.6. Reactant Selectivity 14

Figure 2.7. Product Selectivity 14

Figure 2.8. Transition State Shape Selectivity 15

Figure 2.9. Ship-in-Bottle Synthesis 18

Figure 3.1. Classification of Terpenes 20

Figure 3.2. Conversion of p-cymene to p-cresol via the Hock Process 22

Figure 3.3. Proposed Reaction of α-limonene to Terephthalic acid 22

Figure.3.4. Structure of PET 22

Figure 3.5. Dehydrogenation of Some Monocyclic Monoterpenes 23

Figure 3.6. Proposed Mechanism Leading to p-cymene and Ascaridole 24

Figure 4.1. Structure of Metal Exchanged Zeolite 25

Figure 4.1. Outline of Preparation of Perylene Loaded NaHY 27

Figure 4.2. UV Spectrum of Perylene in 1:3 DCM:Hexane Solution with the Three Maxima Wavelengths 385, 408 and 435 nm 28

Figure 4.3. UV Spectrum of Perylene Loaded NaY with the Characteristic Peaks of Perylene at About 408-435 nm 28

Figure 4.4. Outline of the Terpene Dehydrogenation Procedure 30

Figure 4.5. Outline of the Intrazeolite Photoreaction 31

Figure 4.6. Outline of the Homogeneous System Photooxidation 32

Figure 4.7. Gas chromatogram of a Reaction Product 33

Figure 4.8. GC/MS Chromatogram of p-cymene 33

Figure 4.9. GC/MS Chromatogram of 3-p-menthene 34

Figure 4.10. GC/MS chromatogram of terpinolene isomer 35
Figure 4.11. GC Chromatogram of a RF Standard for the α-terpinene..... 35
Figure 5.1. Disproportionation of α-terpinene in Zeolites 36
Figure 5.2. Acid catalyzed isomerization of α-terpinene 39
Figure 5.3. Disproportionation mechanism of α-terpinene 40
Figure 5.4. Lewis acid catalyzed dehydrogenation of α-terpinen 41
Figure 5.5. UV-Visible spectra of α-terpinene and p-cymene in dried NaHY, and freshly prepared hexane solutions of α-terpinene and p-cymene 44
Figure 5.6. FTIR spectra of NaHY and after reaction with α-terpinene in dried NaHY 44
Figure 5.7. UV-Visible spectra of α-terpinene in dried and calcined NaY, and freshly prepared hexane solutions of α-terpinene and p-cymene 45
Figure 5.8. XRD patterns of NaY, NaHY and NH_4Y vacuum dried at 150 ºC..... 51
Figure 5.9. XRD patterns of dried, non-dried and calcined NaHY..... 52

LIST OF TABLES

Table.2.1. General Characteristics of Several Zeolite Types 11
Table.2.2. Physical Parameters of Zeolite MY 17
Table.3.1. Terpene Nomenclature For Isoprenes 19
Table.5.1. SiO_2/Al_2O_3 Ratio of the Zeolites 37
Table.5.2. Effect of the Type of the Catalyst 37
Table 5.3. EDX Results of the Percent Atomic Contents of NaY, NaHY and NH_4Y, Vacuum Dried at 150 ºC 38
Table 5.4. Effect of the Cation Type 42
Table 5.5. Effect of Drying 46
Table.5.6. Effect of the Amount of The Reactant 47
Table 5.7. Effect of Monoterpene 48
Table 5.8. Irradiation and Sensitizer Effect 48
Table 5.9. Effect of Treating with Pyridine 49
Table 5.10. Effect of Neutralization with Na_2CO_3 50
Table 5.11. EDX Results of the Percent Atomic Contents of NaY, NaHY and Na_2CO_3/NaHY, Vacuum Dried at 150 ºC 50

CHAPTER 1

INTRODUCTION

Dehydrogenations are chemical reactions, which remove hydrogen, and convert saturated single bonds into unsaturated double bonds in organic molecules [1].

Dehydrogenations are important step in the processing of petroleum. Certain petroleums are rich in cycloalkanes, especially methylcyclopentane, 1,2-dimethylcyclopentane, cyclohexane, and methylcyclohexane. These cycloalkanes, called naphthenes in the petroleum industry are intentionally isomerized and dehydrogenated to aromatic hydrocarbons during refining. Aromatic hydrocarbons are important commercial substances and, therefore, this process of catalytic reforming is a major industrial reaction [2].

The dehydrogenation reaction is accompanied by extensive heat absorption. On an industrial scale, the dehydrogenation reaction is generally carried out at a temperature of 550 to 650º C and this reaction is a typical instance of large-energy-consumption type chemical processes. A large quantity of heat energy should be supplied to a reactor for maintaining a high temperature and ensuring much reaction heat [3].

Selective organic dehydrogenation processes is an important reaction type in synthetic organic chemistry. Dehydrogenation of monoterpenes to more valuable aromatic compound p-cymene has commercially importance. The main advantage of the terpenes is being the volatile oil present in trees that can provide an alternative source of hydrocarbon feed stocks that are nonpetroleum based. In the alkylation of toluene and irreversible conversion of terpenes by other synthetic processes for producing p-cymene, has been obtained in relatively low yield or in association with substantial amounts of m-cymene. Since p-cymene is a useful raw material for preparing terephthalic acid for the production of polyester fibers, it is desirable to have a process for producing p-cymene free from the undesirable meta isomer [4, 5, 6].

Conventional catalyzed dehydrogenation reactions are strongly endothermic and large energy is consumed in this type of reactions. In the supported metal or metal oxide catalyzed dehydrogenation of terpenes, applied reaction temperature varies between 150 to 500 ºC. Kirkpatrick [7] carried out dehydrogenation of monocyclic monoterpenes in a container having essentially cupper or silver surfaces with a catalyst of Pd supported activated charcoal at the temperatures between 200 – 400 ºC. Liquori et al. [4, 8] used nickel oxide-molybdenum oxide impregnated silica-alumina as catalyst at the temperatures between 250 – 350 ºC for the conversion of limonene, α-pinene, dipentene and isoprene. Wideman et al. [5, 6] used alkali metal hydroxides and alkali metal carbonates as catalyst supported on silica, aluminum oxide, magnesium oxide, carbon and titanium dioxide, for the dehydrogenation of mono- and bicyclic monoterpenes at a temperature of 300 to 500 ºC. Martin et al. [9] carried out the catalytic aromatization of limonene in the gas phase at 300 to 500 ºC over a catalyst which contains palladium oxide and sulfur, sulfur-selenium or selenium oxide on active carbon. Buhl and Weyrich et al. [10, 11, 12] carried out the conversion of terpenes at temperatures between 200 – 400 ºC by using Ce-promoted Pd catalysts supported on NaZSM-5 zeolite and pure silica impregnated with Pd.

α-Terpinene is one of the mostly used monoterpenes in dehydrogenation reactions. As a proposed methodology it was irradiated in the presence of O_2 and perylene diimide [13] and naphthalene diimide [14] derivatives as photosensitizer in homogeneous system and the main product was the p-cymene. When using the other dyes known to produce singlet O_2, only product was endoperoxide product of α-terpinene. In the absence of O_2 no formation of p-cymene was observed.

These reactions are both performed in homogeneous and heterogeneous systems. Zeolites are very important heterogeneous catalysts that are utilized in hydrocarbon transformations because of its acidity and porosity [15]. The Brønsted acid sites can impart to zeolites a dual behavior as acid and oxidant [16]. Zeolites are microporous crystalline aluminosilicates of different structures, whose physicochemical parameters and chemical composition can be modified by synthesis as well as by post-synthetic treatments. There are more than 300 different zeolites synthesized so far and this offers the possibility to choose among a wide range of different geometries and dimensions of the internal voids [17]. The adsorption of organic molecules containing π electrons,

such as aromatics and olefins, on zeolites results in the formation of radical cations. Strong Lewis acid sites of zeolites are able to abstract an electron from aromatics or olefins to form corresponding radical cation [18]. Spontaneous generation of long-lived organic cation radicals in zeolites has been known for over three decades [16, 17, 19, 20]. The tight fit between the radical cation and the pore size is considered to be the main factor responsible for this stabilization and it is now accepted that the acid sites of zeolites are related to their electron acceptor ability [16].

Generally electron transfer occurs with conjugated systems using NH_4Y, HY and NaZSM-5 as acceptors [21]. Stamires and Turkevich [22] were the first to observe spontaneous electron transfer between the host NH_4Y zeolite and the guests 1,1-diphenylethylene, triphenylamine, quinoline, perylene, aniline and p-phenylene diamine. Ramamurthy et al. [23] have generated and stabilized radical ions from a number of polyenes and oligomers of thiophenes. For example, when activated Na-ZSM-5 (Si/Al = 23) was stirred with α,ω-diphenylpolyenes (trans-stilbene, diphenylbutadiene, diphenylhexatriene, diphenyloctatetraene, diphenyldecapentaene, and diphenyldodecahexaene) in 2,2,4-trimethylpentane, the initially white zoelite and colorless to a pale yellow olefins were transformed into highly colored solid complexes within a few minutes. Diffuse reflectance and EPR results favor the conclusion that the colored species formed upon inclusion of α,ω-diphenylpolyenes in Na-ZSM-5 are long lived radical cations.

In contrast to that acidic zeolites, electron transfer does not spontaneously occur with NaY or NaX, which are susceptible to electron transfer chemistry [21]. Under such conditions, electron deficient sensitizers such as methyl viologen [24, 25] are generally used for photoinduced electron transfer in zeolites. Ramamurthy [26] has reported photoinduced [2+2] dimerizations of arylalkenes sensitized by cyanoaromatic and ionic sensitizers. Furthermore, It has been exploited that the zeolite framework controls the back electron transfer process in the donor – acceptor system – tris(2,2'-bipyridine) ruthenium II ($Ru(bpy)_3^{2+}$) and methyl viologen (MV^{2+}). It has established under that conditions in which the radical ions generated by photoelectron transfer process, live for several hours.

Stratakis et al. [27] carried out intrazeolite photoinduced electron transfer dehydrogenation reactions of α-terpinene within MV^{2+}- supported zeolite NaY system in the absence of a light source (spontaneously) and in inert atmosphere as the first time in the literature. Monoterpene samples were dehydrogenated within MV^{2+}/NaY and stirred either in the dark or by irradiation under argon atmosphere by a non-photochemically driven electron transfer pathway. Non-modified NaY has no effect on the conversion.

In present study, mainly Y type zeolite was used as a combination of electron transfer media and acid catalyst for dehydrogenation reactions of α-terpinene. First of all, cation exchanged and dye-loaded zeolites were prepared. Dehydrogenation reactions and control photooxidation and oxidative dehydrogenation reactions were carried out. Catalytic activity of the Y type zeolite was examined by comparing different types of zeolites.

Before covering the experimental methods, discussion of the results obtained in this study, much more detailed background on zeolites and zeolite-catalyzed dehydrogenation reactions are given.

CHAPTER 2

CATALYSIS
BACKROUND: CATALYSIS AND ZEOLITE CHEMISTRY

2.1. INTRODUCTION

A catalyst is an entity which accelerates a chemical reaction without being consumed itself in the process. Without catalysts, various chemical reactions of great importance would proceed so slowly that they could not even be detected, although the reaction conditions (temperature and pressure) are thermodynamically favorable for the occurrence of the reactions. Suitable catalysts provide a solution to this problem. They make it possible for the reactions to proceed at rates high enough to permit their commercial exploitation on a large scale, with resulting economic benefits for everyone [28]. This property makes both homogeneous and heterogeneous catalysts vital in organic chemistry.

Homogeneous catalysis is generally defined where the reactant molecules and the catalyst are present in a single phase, as in a liquid solution. Acid and base catalyses are the most important types of homogeneous catalysis in liquid solution.

On the other hand in heterogeneous catalysis, the reactants are present in the one phase and the catalyst in another, with the catalytic action occurring at the interface or surface between them. Usually the catalyst is a solid and the reactants are either gases or liquids [28].

Nowadays, the chemical industry is under increased pressure to develop cleaner production processes and technologies. Much effort is devoted to the development of heterogeneous catalysts, their application in industrial-scale organic synthesis of fine chemicals and the abatement of pollutants that are detrimental to the environment [29, 30].

Zeolites have been playing a role in heterogeneous catalysis. An impressive number of large-scale industrial processes in petroleum refining, petrochemistry and the manufacture of organic chemicals are carried out using zeolite catalysts. Altogether, zeolite catalysis has become a most important sub-field of heterogeneous catalysis [31].

2.2. ZEOLITES AS HETEREGENOUS CATALYSTS

Zeolites occur in nature and have been known for almost 250 years as aluminosilicate minerals. Today, zeolite structures are of great interest in catalysis. Because of changing in their chemical composition from one deposit to another and even from one stratum to another in the same deposit, containing almost always undesired impurity phases and not optimized properties for catalytic applications, catalytic perspective, naturally occurring forms of zeolites are of limited value [32].

On the other hand, synthetic zeolites have been encountering a growing interest because of their applications as catalysts in industry, and for this reason there are currently massive efforts in trying to synthesize new kinds of zeolite-type materials [33].

Synthetic zeolites were first introduced as catalysts for large-scale gas phase reactions in petrochemistry. Reactions such as cracking and aromatic isomerisation and disproportionation, showed the advantages of zeolites compared to conventional liquid acids in terms of easy separation of the reaction mixture, reactor design, control of the outcome of the reaction, shape selectivity effects, and the possibility to regenerate the catalyst after deactivation. The results of the gas-phase reactions triggered an intense research aimed at developing the potentialities of zeolites for general acid-catalyzed organic reactions in the liquid phase under batchwise conditions. During the last two decades an increasing number of publications have appeared reporting the use of zeolites as solid catalysts for organic reactions in the liquid phase for the production of fine chemicals [34, 35].

2.3. ZEOLITES

In 1756, the Swedish mineralogist Cronstedt discovered the mineral stilbite. He called this mineral and other certain silicate minerals ‘zeolite’ in allusion to their behavior on heating in a borax bead, (Greek zeo = boil; lithos = stone) because many zeolites appear to boil when heated. Since then, zeolites have been recognised as a separate group of minerals, one of the most abundant on earth, and 48 separate species have been discovered so far. The synthesis of zeolites has first been reported at 1862, but the synthesized products could not be assigned completely until the 1930s. The first crystalline structure determination of a zeolite was established on analcime (Taylor, 1930); following this, Hey (1930) concluded that zeolites in general have aluminosilicate frameworks with loosely bonded alkali or alkali-earth cations, or both. In 1956, the first fully characterized synthesis of a zeolite not occurring in nature was reported, and many others have followed in its wake [36, 37].

Approximately 40 natural zeolites have been identified over the past 200 years, the most common of which are analcime, chabazite, clinoptilolite, erionite, ferrierite, heulandite, laumontite, mordenite, and phillipsite. More than 300 zeolites have been synthesized. Some of the more common synthetic zeolites are zeolites A, X, Y, β, ZMS-5, MCM-41 and Mordenite. Natural and synthetic zeolites are used commercially because of their unique adsorption, ion-exchange and molecular sieve properties as water softeners in detergents, as catalysts, as adsorbents or desiccants, or even as soil improvers, to control soil pH, moisture, and manure malodour. Zeolite research covers an even wider area, including catalytic and ion exchange properties of zeolites, zeolite synthesis and the behavior of molecules adsorbed on the zeolite surface [36, 38].

2.4. STRUCTURAL FEATURES OF ZEOLITES

2.4.1. Zeolite Framework Structure

Zeolites are a group of crystalline aluminosilicates, with group I or II elements (e.g. Na, K, Ca, Mg) as counterions. They consist of a framework of $[SiO_4]^{4-}$ and $[AlO_4]^{5-}$ tetrahedra, linked to each other at the corners by sharing all of the oxygens.(Figure 2.1.) Represented empirical formula for zeolites:

$$M_{2/n}O{\cdot}Al_2O_3{\cdot}xSiO_2{\cdot}yH_2O$$

In this formula, n is the cation valence (typically Na, Ca, Mg, etc.), *x* is the SiO_2/Al_2O_3 ratio and *y* is the water content in the hydrated zeolite. The tetrahedra make up a three-dimensional network, with lots of open spaces as channels or interconnected voids that occupied by cations and water molecules. The cations are mobile and undergo ion exchange. It is these voids that define the many special properties of zeolites, such as the adsorption of molecules on the huge internal surface (between 500 and 1000 m^2/g) [31, 36, 39].

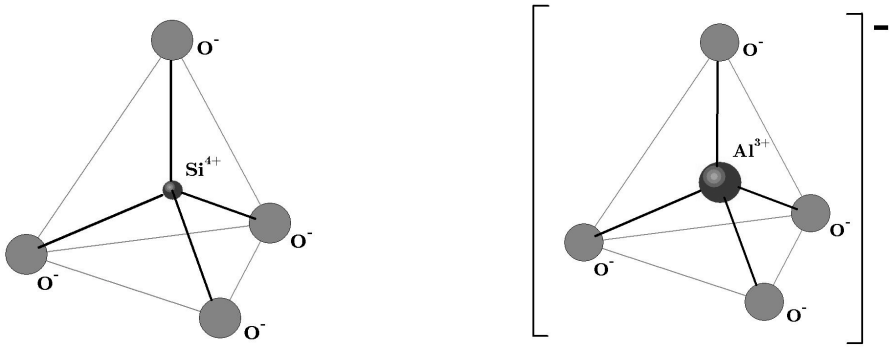

Figure 2.1. Silica and Alumina Tetrahedra

The framework of a zeolite contains channels, channel intersections and/or cages with dimensions between 0.2 and 2 nm. Inside these voids are water molecules and small cations, which compensate the negative framework charge. The chemical composition of a zeolite can hence be represented by a formula of the type (e.g. for zeolite Y $M_{56}(AlO_2)_{56}(SiO_2)_{136} \cdot 253H_2O$) [32, 40].

2.5. ZEOLITE PROPERTIES

2.5.1. Pore Structure And Molecular Sieving

Perhaps the most unique feature zeolites have is their ability to act as molecular sieves. Within the supercages, guest molecules can reside. The strictly defined, uniform shape and size of these cages makes sure only molecules of a certain size or smaller can penetrate within the zeolite and adsorb there. This property allows for the very efficient use of zeolites in separation processes. Other materials, such as alumina, carbon, or porous glass, have molecular sieve properties as well, but none so versatile as zeolites have. The main reason for this is the poor pore size distribution in these other materials, as shown in Figure 2.2. Within one zeolite species, pore size is very narrowly defined, but the wide range of available zeolites allows for a wide variety in pore size.

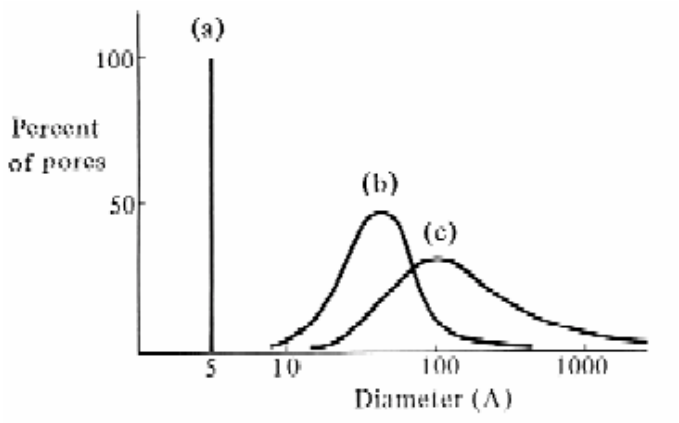

Figure 2.2. Pore size distribution in some adsorbents. (a) Dehydrated zeolite; (b) silica gel; (c) activated carbon [36].

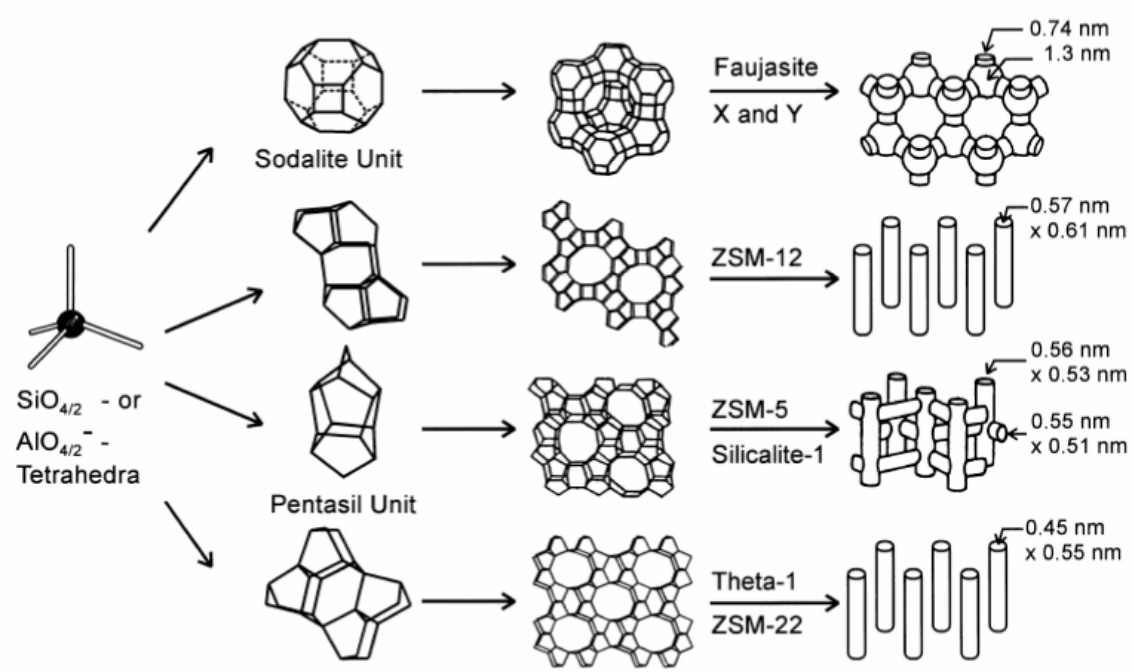

Figure 2.3. Pore topology of some common zeolites [32].

Depending on the preparative method used, several predictable 3-dimensional zeolite structures are obtained. There are mainly two types of pore structure of zeolites (Figure 2.3). One of them, faujasites, provides an internal pore system comprised of interconnected cage like voids, (e.g. zeolites X/Y and A) and their basic structure is the sodalite cage. The other, pentasils, provide a three dimensional system of uniform channels (e.g. zeolite beta, mordenite, and ZSM-5). Zeolites that are commonly used for synthetic transformations include zeolites X/Y, beta, mordenite, and ZSM-5. Zeolite A, whose pore dimensions preclude adsorption of larger molecules, is typically used only as a water scavenger [21].

Table 2.1. General Characteristics of Several Zeolite Types [21].

Zeolite	Pore type	Dimensions	Commercial products	Si/Al ratio, cation present	Molecules absorbed
Zeolite A (LTA)	Interconnected spheres	4.1Å diameter pore 11.4Å diameter cavity	Linde Type 4A, 3A, 5A molecular sieves	1, Na^+ Na^+/K^+, Na^+/Ca^+	water, methanol
Zeolite X/Y (Faujasite, FAU)	Interconnected spheres	7.4Å diameter pore 11.8Å diameter cavity	13X, CBV-100, HSZ-320NAA CBV-400 HSZ-390HUA	5, Na^+ 5, H^+ 200, H^+	naphthalene various steroids
ZSM-5 (MFI)	Interconnected channels	5.3 x 5.6Å channel 5.1 x 5.5Å channel	CBV-3020 CBV-30014	30, H^+ or NH_4^+ 300, H^+ or NH_4^+	cyclohexane biphenyl
Mordenite (MOR)	Interconnected channels	6.5 x 7Å channel 2.6 x 5.7Å channel	HSZ-620HOA CBV-10A HSZ-690HOA	15, H^+ 13, Na^+ 200, H^+	neopentane
Zeolite beta (BEA)	Interconnected channels	7.6 x 6.4Å channel 5.5 x 5.5Å channel	CP-811BL-25	25, H^+	*cis*-4-*tert*-butyl cyclohexanol

Most common used zeolite; faujasite framework has two main structural features. The main supercage is a result of assembly of the basic unit 'sodalite cage'. While sodalite cages are too small to accommodate organic molecules, the spherical supercages are about 13Å diameter. Access to the supercages is afforded by four 12-ring windows about 9Å in diameter. There are four windows tetrahedrally distributed about the center of the supercage. The supercages form a three-dimensional network with each supercage connected tetrahedrally to four other supercages through the 12-membered ring window. (Figure 2.4.a) Hence, one should not view X and Y zeolites as a crystalline material consisting of independent supercages. All supercages are open and are interconnected to four others. A unit cell of X and Y zeolite consists of eight supercages [26].

a) b)

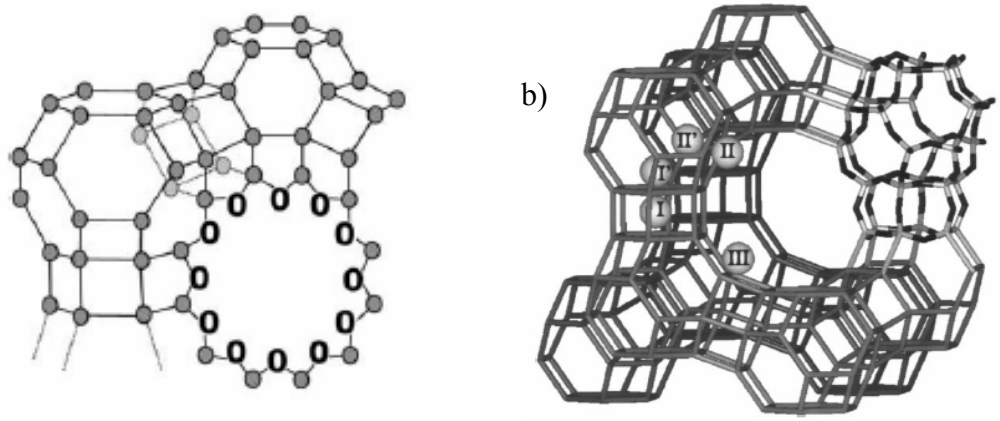

Figure 2.4. a) 12-Membered Ring Window [41] and b) Cation Locations in Faujasite-type Zeolites [33].

Charge-compensating cations present in the internal structure of zeolites are known to occupy three different positions (Figure 2.4.b) in zeolites X and Y; the first type (site I) with 16 cations per unit cell (both X and Y) is located on the hexagonal prism faces between the sodalite units. The second type (site II) with 32 per unit cell (both X and Y) is located in the open hexagonal faces. The third type (site III) with 38 per unit cell in the case of X-type and only eight per unit cell in the case of Y-type is located on the walls of the larger cavity. Only cations at sites II and III are expected to be readily accessible to the organic molecule adsorbed within a supercage [26].

2.5.2. Acidic And Basic Character Of Zeolite

Hydrocarbon transformations utilizing the acidity and pores of zeolites are very important in petroleum industry. The acidity of zeolites has been extensively studied by spectroscopic methods and theoretical approaches [15]. Zeolites also have amphoteric properties, dual involvement of acidic and basic sites that are present in the zeolite structure [21, 41, 42, 43]. The bridging Si–OH $\cdots$ Al group is usually referred to as a Brønsted acid site in zeolites. On the contrary, no basic framework OH group has been reported to exist. Zeolites contain Lewis as well as Brønsted acid sites. The three-coordinated aluminum sites on the framework and non-framework Al sites are normally considered to be Lewis sites.

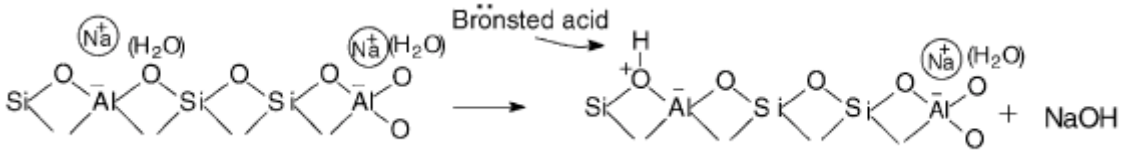

Additionally, charge-compensating cations act as Lewis acids, while the framework oxygens represent a base. In particular, the oxygens adjacent to Al (Si–O–Al oxygens) are more basic because of a larger negative charge on oxygen.

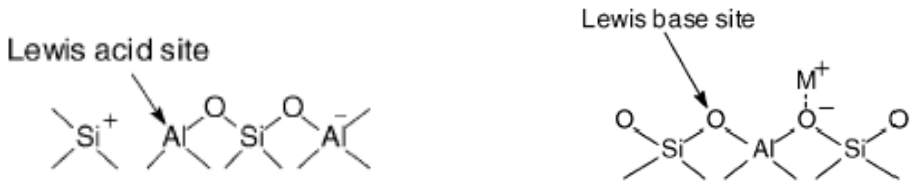

The Lewis acidity is usually connected to an electron accepting property, and the basicity to an electron-donating property. Thus, the zeolites behave both as electron donors and as acceptors of moderate strength to the guest species, depending on the adsorption site. As a rule, the acid strength or the electron-accepting ability increases with increasing Si/Al ratio and for zeolites with smaller alkali metal cations ($Li^+ > Na^+ > K^+ > Rb^+ > Cs^+$). For example, Li^+-Y is more acidic than Cs^+X. On the other hand, the basic strength (electron-donating ability) of the zeolites increases with decreasing Si/Al ratio and for zeolites with larger alkali metal cations. In this regard, Cs^+X is more basic than Li^+-Y. Accordingly, the chemical properties of the zeolites can be fine-tuned in terms of composition, cations and framework structure [41].

Brønsted acid sites are generated by the aqueous ion exchange with an ammonium salt followed by thermal decomposition of the ammonium ions inside the zeolite (Figure 2.5.). Upon severe heat treatment (>500ºC), the Brønsted acid sites are degraded ('dehydroxylation'), water is split off with the concomitant formation of Lewis acid sites [32].

$$NH_4^+ + Na^+Z^- \xrightarrow[-\,Na^+]{} NH_4^+Z^- \xrightarrow[-\,NH_3]{\sim 300\text{-}400^oC} H^+Z^-$$

Figure 2.5. Formation of Brønsted Acid Sites

Depend on the studies of Ramamurthy et al. [44] among on faujasite type zeolites, CaY, HY, and NaY contain Brønsted acid sites. Of these HY, as expected, contains the most acidic protons (42–47 per unit cell). This is followed by CaY activated in an oven which contains 16 per unit cell. Even NaY, normally considered to be non-acidic, contain 0.5 protons per unit cell. The acidity of CaY depends on the activation conditions and that of NaY depends on the source. NaX is least acidic one. In choosing X and Y zeolites as a reaction media it is important to be aware of the consequences of the presence of even small numbers of Brønsted acid sites in CaY, HY, and NaY zeolites and these are large enough to bring about changes in the structure of guest alkenes via a catalytic process.

2.5.3. Shape Selectivity

The combination of high internal surface area, strong acid sites, selective sorption and molecular sieving properties makes zeolites among the most useful and versatile heterogeneous catalysts. High internal surface area and acidity give rise to high activity, while selective sorption and molecular sieving result in high reaction selectivity. Reaction selectivity may be diffusion controlled (reactant or product selective) or may be geometrically controlled (transition state selective) [45].

1) Reactant selectivity: From a mixture of reactants, only those of the appropriate dimensions will enter the zeolite cavity and undergo chemical transformation. A classic example is the selective cracking and adsorption of n-alkanes from paraffin mixtures (Figure 2.6.).

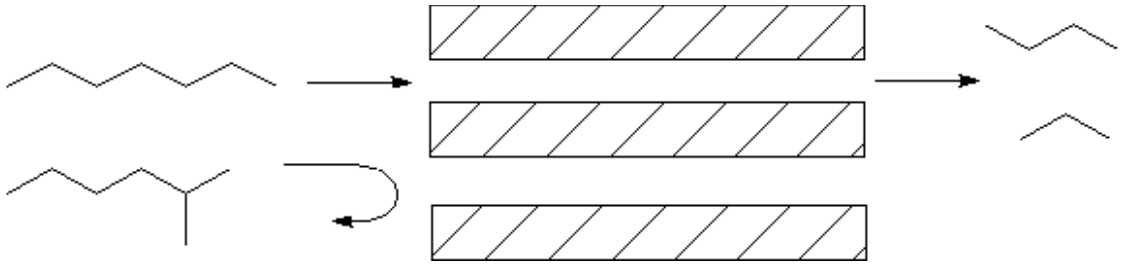

Figure 2.6. Reactant Selectivity

2) Product selectivity: From a mixture of products formed during the zeolite-catalyzed reaction, only those of appropriate dimension may diffuse out of the pores. An important application of this process is seen in zeolite-mediated electrophilic aromatic substitutions, exemplified by the para-selective Friedel-Crafts monoalkylation of toluene using zeolite ZSM-5 (Figure 2.7.).

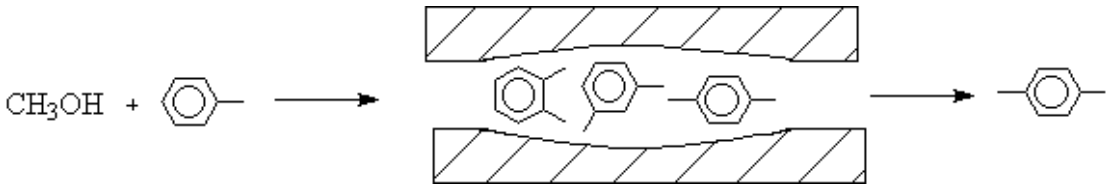

Figure 2.7. Product Selectivity

3) Transition state shape selectivity: This last type of selectivity, also termed restricted transition state selectivity, requires the reaction to occur either at or within the zeolite pore. Similar to enzyme catalysis, the zeolite will stabilize one transition state over another, either by size or shape effects (Figure 2.8.).

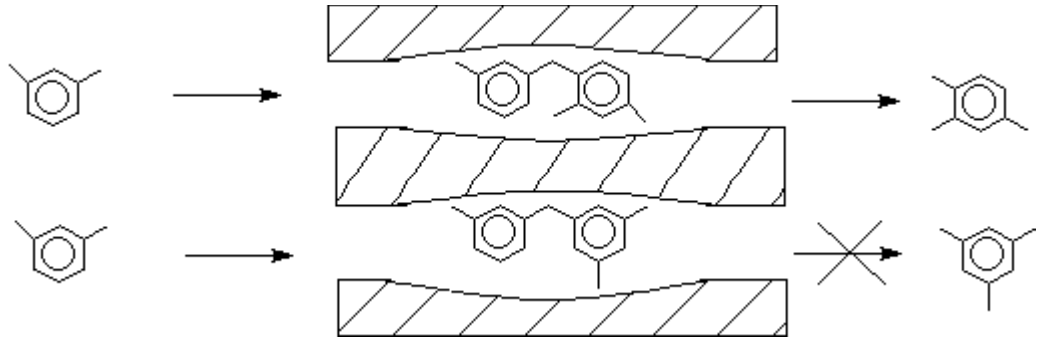

Figure 2.8. Transition State Shape Selectivity

Thus, by one or more of the above methods, zeolites can control the selectivity of chemical transformations, by changing either the products formed or the ratio of the product(s) formed [21, 45].

Modification of the shape selective properties of zeolites is possible with different approaches for catalytic purposes. Most of these approaches not only change the shape selective but also the acid properties of zeolites. It is in fact impossible to change these properties independently. These approaches are given as follows [46]:

(i) Cation exchange: Small cations like H^+ and Na^+ can be replaced by larger cations such as K^+, Rb^+, Cs^+, using the ion-exchange method. This replacement results in the narrowing of the pore diameter of the zeolite channels in addition to a change in the number and strength of the Brønsted acid sites.

(ii) Deposition of inorganic oxides: By deposition of inorganic oxides in the pores of the zeolite, the effective pore diameter is reduced and the steric constraints on reactants, transition state or products are enhanced. Deposition of these oxides also changes the acidic and basic properties of the zeolite.

(iii) Crystal size: The crystal size of zeolite catalysts can be varied by adapting the synthetic conditions. By increasing crystal size, the fractional amount of sites on the outside of the crystal in comparison to the total amount of sites decreases and consequently the center of catalytic activity shifts from extra to intrazeolitic.

(iv) Deactivation of the external surface: For small crystals, the active sites on the external surface largely contribute to the catalytic activity of the material. In the case of Brønsted acid sites, they can be deactivated by deposition of inorganic oxides or neutralized by chemical reaction with organosilanes which are too bulky to diffuse through the intracrystalline voids. By silylation, the hydrophobicity of the materials is enhanced.

(v) Deposition of organic bases: Deposition of organic bases in the intracrystalline voids narrows the pore apertures and so enhances the steric constraints on molecular diffusion.

2.5.4. Ion Exchange

The properties of individual zeolites depend upon (i) the framework structure (size, shape, tortuosity, interconnectivity of channels and cages) (ii) Framework composition (concentration and distribution of framework isomorphous substitutions) (iii) Intracrystalline cations (charge, type, concentration, location) (iv) Additional phases (e.g. non-framework oxides, impregnated metals, intercalated organic compounds, etc.) Zeolite properties can be changed with modification by cation exchange (e.g. to introduce protons, forming solid acids), impregnation (e.g. with platinum group metals), etc. These modifications give rise to a diverse range of physical and chemical properties, allowing zeolites to be adapted for numerous applications [45].

Cations are located in the zeolite framework, mobile and occupy various exchange sites depending upon their radius, charge, and degree of hydration. Through ion exchange, other metal ions can be introduced; this might influence the supercage size, thereby modifying the molecular sieving or catalytic properties of the zeolite. These are selected from the group comprising alkali metals such as hydrogen, lithium, sodium, potassium, cesium and rubidium, alkaline earth elements, such as magnesium,

calcium, barium and strontium and transition elements such as lanthanum. The pore size of zeolite A, about 4 Å, is reduced to about 3 Å when the Na^+ ion is replaced by the larger K^+, and enlarged to about 5 Å when Ca^{2+} is introduced instead. However, if suitable, any cation may be used. While zeolites are preferred, any porous solid material with molecular size cages featuring strong electrostatic fields may be used [36, 47] (Table 2.2.).

Table 2.2. Physical Parameters of Zeolite MY [36].

cation	cation ionic radius (Å)	electrostatic field within supercage (V/Å)	vacant space within supercage ($Å^3$)
Li^+	0.76	2.1	834
Na^+	1.02	1.3	827
K^+	1.38	1.0	807
Rb^+	1.52	0.8	796
Cs^+	1.67	0.6	781

The cation exchange behavior of zeolites depend upon [39]:

i. The nature of the cation species, the cation size, both anhydrous and hydrated and cation charge,
ii. The temperature,
iii. The concentration of the cation species in solution,
iv. The anion species associated with cation in solution,
v. The solvent,
vi. The structural characteristic of the particular zeolite.

Usually, ion exchange is applied by simply contacting the zeolite with a salt solution of a different cation at ambient temperature, or at elevated temperature if an accelerated exchange rate is desired. The exchange reaction, in which one type of cation is replaced with another, assumes an equilibrium state that is specific to the particular zeolite and particular cations [48].

2.5.5. Ship-In-A-Bottle Synthesis

In addition to ion exchange, another way to incorporate the desired molecule onto the zeolite is ship-in-a-bottle synthesis. Neutral molecules, such as arene electron acceptors, can easily be adsorbed by bringing the compound in contact with the zeolite, usually in a solvent like hexane. This works fine for small molecules. However, as we have seen, the supercages of the faujasite supercages are about 13 Å across, but the windows giving access to these cages are only 7.4 Å wide. Larger molecules, that might be accommodated within the supercage, cannot be introduced because they cannot enter. To overcome this difficulty, the desired molecules can be synthesized within the zeolite framework, from building blocks that are small enough to diffuse through to the inside. Of course, the synthesized molecules can neither leave nor relocate within the zeolite; they are completely locked in place (Figure 2.9.). This is called ship-in-a-bottle synthesis, by analogy to the little ships built by sailors that apparently never could have entered their bottles [36].

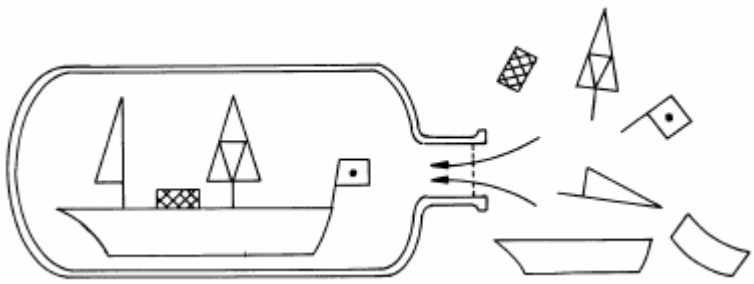

Figure 2.9. Ship-in-Bottle Synthesis [49]

CHAPTER 3

INTRAZEOLITE DEHYDROGENATION OF TERPENES TO p-CYMENE

3.1. TERPENES

Terpenes are a group of unsaturated aliphatic cyclic hydrocarbons, which, unlike petroleum distillates, are derived from plants as constituents of essential oils. They derive from the head-to tail linkage of the ‘‘isoprene’’ moiety and have carbon ranges from C_{10} to C_{40}. Isoprene, 2-methyl butadiene, has a conjugated diene structure, $CH_2=C(CH_3)CH=CH_2$. Many terpenes are hydrocarbons, but oxygen-containing compounds such as alcohols, aldehydes or ketones (terpenoids) are also found. The ‘‘terpene’’ nomenclature of these compounds is shown in Table 3.1. [50, 51].

Table 3.1. Terpene Nomenclature For Isoprenes

Carbon atoms	Isoprene units	Nomenclature
10	2	Monoterpenes
15	3	Sesquiterpenes
20	4	Diterpenes
25	5	Sesterterpenes
30	6	Triterpenes
40	8	Tetraterpenes

Monoterpenes may be acyclic, monocyclic, or bicyclic as can be seen in Figure 3.1. Their distinguishable isomers can differ only by as much as the positioning of a double bond within a ring (e.g., α- and γ -terpinene) and there exist optical isomers of some (e.g., limonene). In general, they are high boiling point oils, but they do have significant vapour pressures at room temperature [51].

Terpenes have limited chemical stability, as a result of photolysis, oxidation and other reactions; e.g., the atmospheric chemical lifetime of monoterpenes under daylight conditions was estimated to range from less than 5 min (α-terpinene) to 3 hours (α- and β-pinene, sabinene) [52]

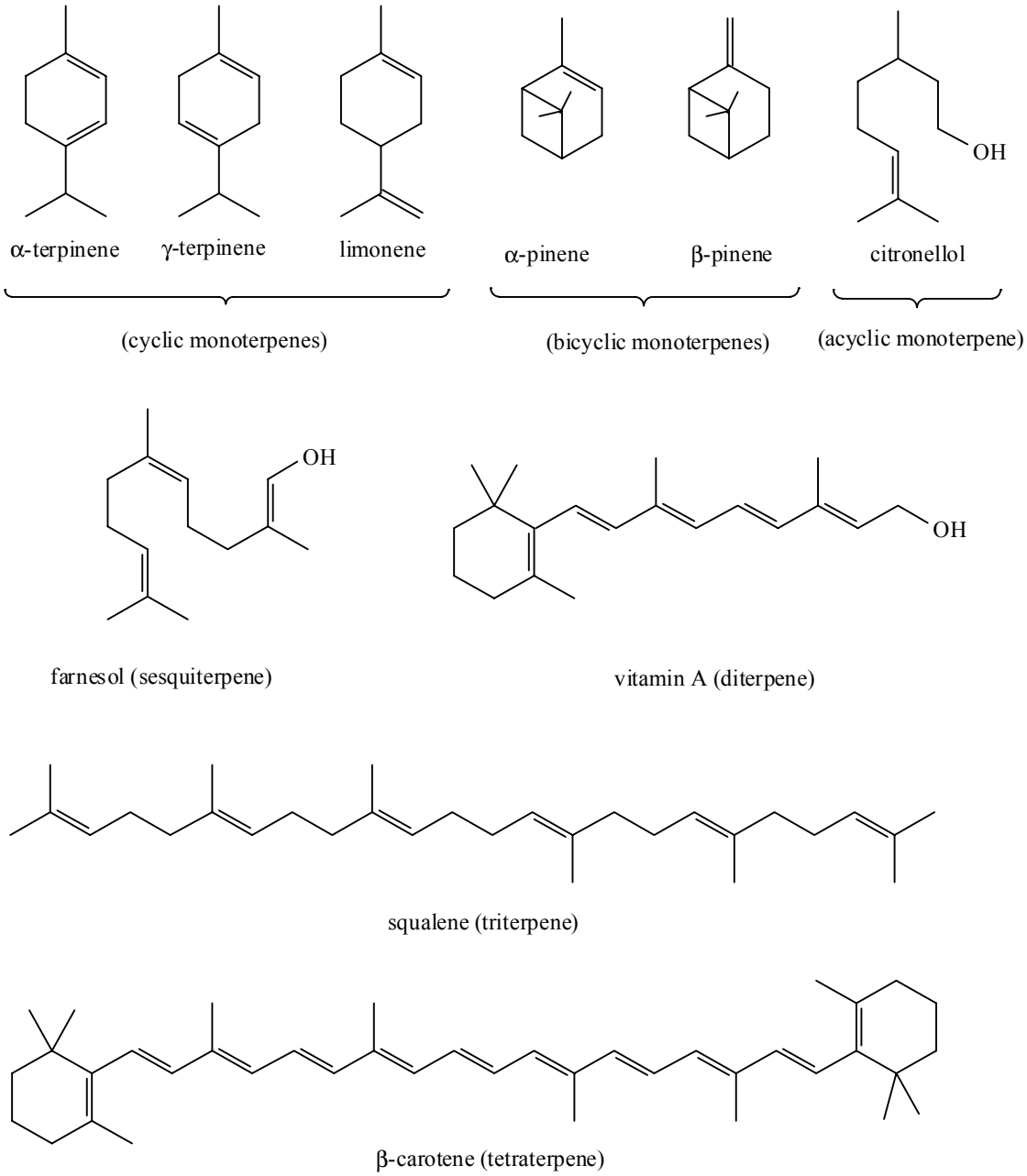

Figure 3.1. Classification of Terpenes

Terpenes are renewable hydrocarbon source that widely and cheaply available as by-products from the orange and lemon juice production and in spices and natural aromas as well as from pulp and paper industry. Their main advantage is being the volatile oil present in trees that can provide an alternative source of hydrocarbon feed stocks that are nonpetroleum based [5, 11, 12, 51, 53].

The technologically important reactions of terpenes are of six main types [54]:

1) Acid-catalyzed rearrangements, additions, and eliminations
2) Thermal rearrangements
3) Allylic rearrangements
4) Hydrogenations and other reductions, and dehydrogenations
5) Stereochemical changes (epimerization)
6) Oxidations, including halogenations

3.2. DEHYDROGENATION OF TERPENES TO p-CYMENE

3.2.1. Industrial Importance of p-Cymene

p-Cymene is of high interest as an important intermediate used in pharmaceutical and fragrance industry and for the production of fungicides, pesticides, as flavoring agent and as a heat transfer medium and it is also a raw material for the synthesis of non-nitrated musks, which nowadays tend to replace nitrated ones [11, 12, 55].

p-Cymene is also used as an important starting material for the production of p-cresol. Currently, amongst other methods p-cresol is manufactured via the Hock process (Figure 3.2.), the same process that is used worldwide to produce phenol. Starting from p-cymene (isopropyltoluene) the process involved a peroxy intermediate, producing p-cresol and acetone [56].

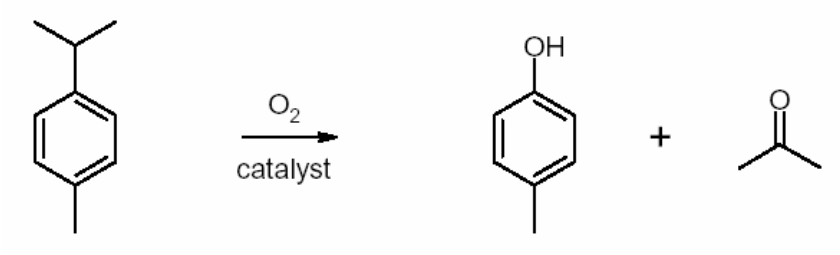

Figure 3.2. Conversion of p-cymene to p-cresol via the Hock Process [56]

p-Cymene is also used for the formation of polymers (synthetic fibers, antiseptics, etc.). Starting from terephthalic acid, by the oxidation of p-cymene (Figure 3.3.), which in turn can be produced from the dehydrogenation of limonene, poly(ethylene terephthalate) can be produced.

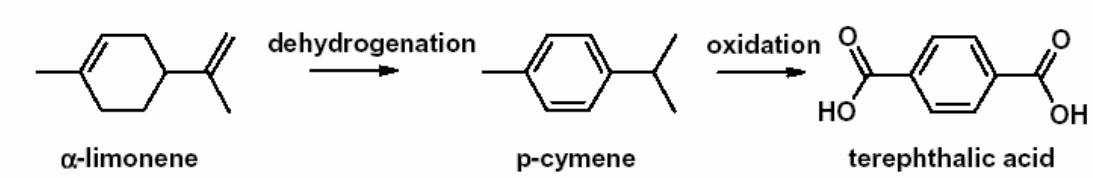

Figure 3.3. Proposed Reaction of α-limonene to Terephthalic acid [56].

By the direct esterification of terephthalic acid and ethylene glycol or by trans esterification of dimethyl terephthalate with ethylene glycol, poly-ethylene terephthalate (Figure 3.4.) can be prepared. In both cases the starting materials are currently petroleum derivatives [56].

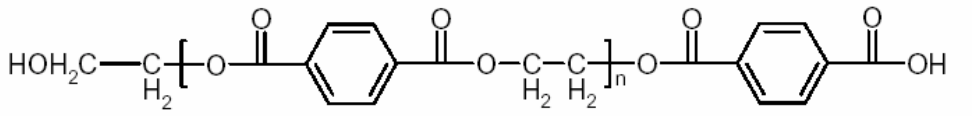

Figure 3.4. Structure of PET [56]

3.2.2. Production of p-Cymene

Dehydrogenation of various terpenes over homogeneous and heterogeneous catalysts [4, 5, 6, 7, 8, 9, 10, 11, 12, 57, 58] and isopropylation of toluene [55, 59] has been investigated for the production of p-cymene thoroughly in the past.

Some monocyclic monoterpenes (limonene, α-phellandrene, terpineol, carveol) (Figure 3.5.) are dehydrogenated by N-Lithioethylenediamine solution to p-cymene in homogeneous media. The solution formed from the reaction of lithium with ethylenediamine, which probably contains $H_2NCH_2CH_2NHLi$, is capable of rapidly and quantitatively isomerizing a terminal olefin to an internal olefin. Monoterpenes are converted to the corresponding aromatic hydrocarbon, with evolution of hydrogen gas; this reaction takes place slowly even at room temperature. The corresponding sodium compound, $H_2NCH_2CH_2NHNa$, isomerizes olefinic double bonds at a very slow rate; however it will rapidly aromatize monoterpenes in which the double bonds are already conjugated and in the ring [57].

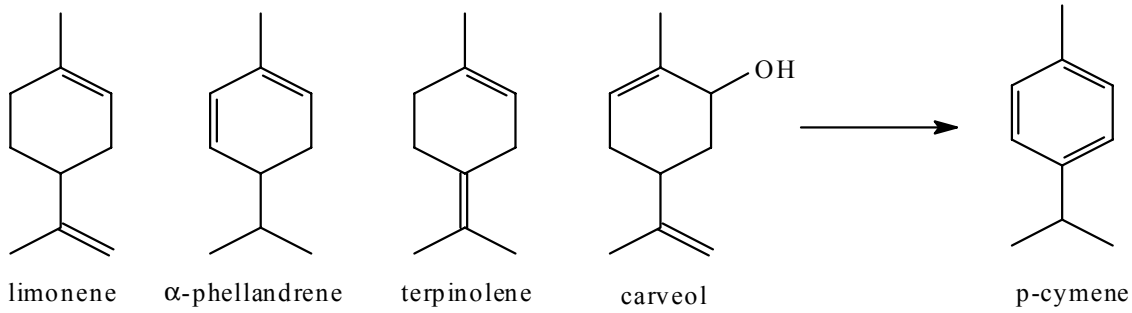

Figure 3.5. Dehydrogenation of Some Monocyclic Monoterpenes

It is also proven that monoterpenes can also be converted to their dehydrogenated derivatives in the presence of various photosensitizers e.g., perylene or naphthalene diimides under irradiation, through a singlet state electron transfer in an exciplex, that forms hydroperoxy radicals reaching to p-cymene in radical chain reactions [13, 14].

As stated before in the introduction part, it has been shown that monoterpene disproportionates over noble metals in particular Pd-containing catalysts, to p-menthane and p-cymene by using various heterogeneous systems. It was proved that the acidity has no real influence on the reaction pathway and that a purely hydrogenation/dehydrogenation mechanism takes place. Indeed, the isolated double bonds of monoterpene can be hydrogenated rapidly in the presence of hydrogen. Equilibrium is afterwards established between p-menthane and p-cymene that is a

function of temperature and hydrogen pressure. At temperatures of 300 ºC, the yield of p-cymene is nearly 95-99% [10, 11, 12].

Several monoterpenes loaded within the Methyl viologen-supported NaY and are dehydrogenated to p-cymene in the absence of an irradiation source (spontaneously). The reaction occurs even in the open air with formation of minor amounts of ascaridole depending on the substrate (Figure 3.6.). It is proposed that the radical cations of the monoterpenes are formed by single electron transfer to NaY, with methyl viologen acting as a promoter [27].

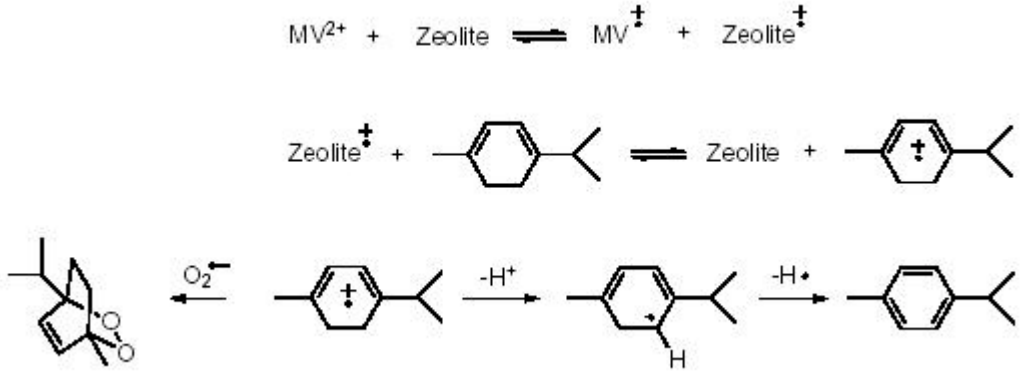

Figure 3.6. Proposed Mechanism Leading to p-cymene and Ascaridole [27].

Recently, it was shown that several monoterpenes (monocyclic, bicyclic or acyclic) isomerize and finally transform to p-cymene in the dark upon loading within thionin-supported zeolite NaY. The same reactions occur in NaY dried under the same conditions as thionin/NaY. It is postulated that the thermal treatment of NaY generates ‘electron holes’ (probably acidic sites). The transformation of monoterpenes occurs more likely via an electron transfer-induced reaction subordinated to the occurrence of the acidic sites. The radical cation of the more thermodynamically stable monoterpene, α-terpinene, eventually dehydrogenates to p-cymene. For comparison, the same reactions were performed within methyl viologen-supported NaY [60].

CHAPTER 4

EXPERIMENTAL STUDY

4.1. PREPARATION OF CATION EXCHANGED ZEOLITES

4.1.1. Preparation of NaHY

Sodium cations were loaded into the zeolite by stirring 25 g of NH_4Y zeolite (Zeolyst International, CBV 500, SiO_2/Al_2O_3 mole ratio: 5) in 250 mL 10 % $NaNO_3$ (Carlo Erba >99%) solution by refluxing over 24 h. Following the ion-exchange process, the zeolite suspension was filtered, washed thoroughly by ultra pure water and this process repeated three times. Finally zeolite was dried at 120 °C overnight.

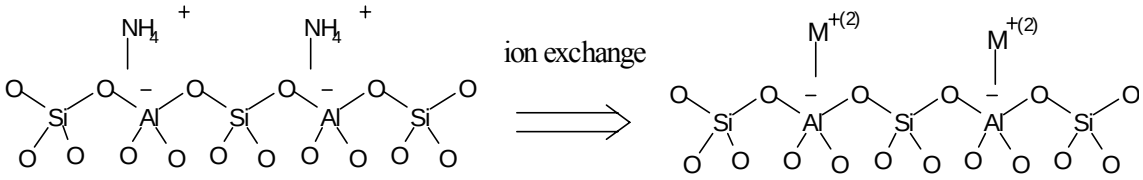

Figure 4.1. Structure of Metal Exchanged Zeolite

4.1.2. Preparation of LiHY, KHY and CaHY

Metal cations were loaded into the zeolite by stirring 5 g of NH_4Y zeolite in 50 mL 10 % corresponding metal chloride or metal nitrate solution by refluxing over 24 h. Following the ion-exchange process, the zeolite suspension was filtered, washed thoroughly by ultra pure water and this process repeated three times. Finally zeolite was dried at 120 °C overnight.

4.1.3. Preparation of CsNaY

Cesium cations were loaded into the zeolite by stirring 10 g of NH_4Y zeolite in 50 mL of 0.3 M cesium chloride (Merck >99.5%) solution at 80°C for 24 h. The zeolite suspension was filtered, washed thoroughly by ultra pure water and this process

repeated three times. Cesium exchanged zeolite was dried at 120 °C overnight after the ion exchange process.

4.1.4. Preparation of CsNaX

Cesium cations were loaded into the zeolite by stirring 3 g of NaX (Aldrich, 28,359-2 Molecular Sieve 13X, powder) zeolite in 30 mL of 0.3 M cesium chloride solution prepared with ultra pure water, degassed with Ar, at room temperature for 24 h under Ar atmosphere. The zeolite suspension was filtered, washed thoroughly by degassed ultra pure water under Ar and this process repeated three times. Cesium exchanged zeolite was dried at 80 °C overnight under vacuum after the ion exchange process.

4.1.5. Preparation of LiNaHY, CaNaHY and KNaHY

Metal cations were loaded into the zeolite by stirring 3 g of NaHY zeolite in 30 mL 10 % corresponding metal chloride or metal nitrate solution by refluxing over 24 h. Following of the ion-exchange process the same method as in the procedure was applied for the preparation of Li, Ca and K exchange of NH_4Y.

4.1.6. Preparation of HY

HY zeolite was obtained by the calcination of NH_4Y-zeolite at 550°C for 10 h in air atmosphere.

4.1.7. Preparation of Calcined NaHY and NaY

NaHY and NaY (Zeolyst International, CBV 100, SiO_2/Al_2O_3 mole ratio: 5) was calcined at 550°C for 10 h in air atmosphere.

4.1.8. Preparation of NaHβ and NaHMOR

Sodium cations were loaded into the zeolite by stirring 5 g of NH_4-β (Beta, Zeolyst International, CP-814E, SiO_2/Al_2O_3 mole ratio: 25) and NH_4-MOR (Mordenite,

Zeolyst International, CBV 21A SiO_2/Al_2O_3 mole ratio: 20) zeolite in 50 mL 10 % $NaNO_3$ (Carlo Erba >99%) solution by refluxing over 24 h. Following the ion-exchange process, the zeolite suspension was filtered, washed thoroughly by ultra pure water and this process was repeated three times. Finally zeolite was dried at 120 °C overnight.

4.1.9. Preparation of Perylene Loaded NaHY

2 g NaHY was dried at 250 °C overnight under vacuum. Dried NaHY was poured into a 100 mL two necked round-bottom flask under Ar atmosphere and then immediately 50 mL of 1:3 dichloromethane:hexane mixture solution of 2.4 mg perylene was added. Zeolite-dye suspension was stirred for three days. Then brownish suspension was filtered and washed with the same solvent mixture until the washing filtrate solution had no UV-Visible absorption. Figure 4.1 shows the schematic representation of the reaction procedure. Also UV-Visible spectrum of the perylene/NaHY was confirmed the loading.

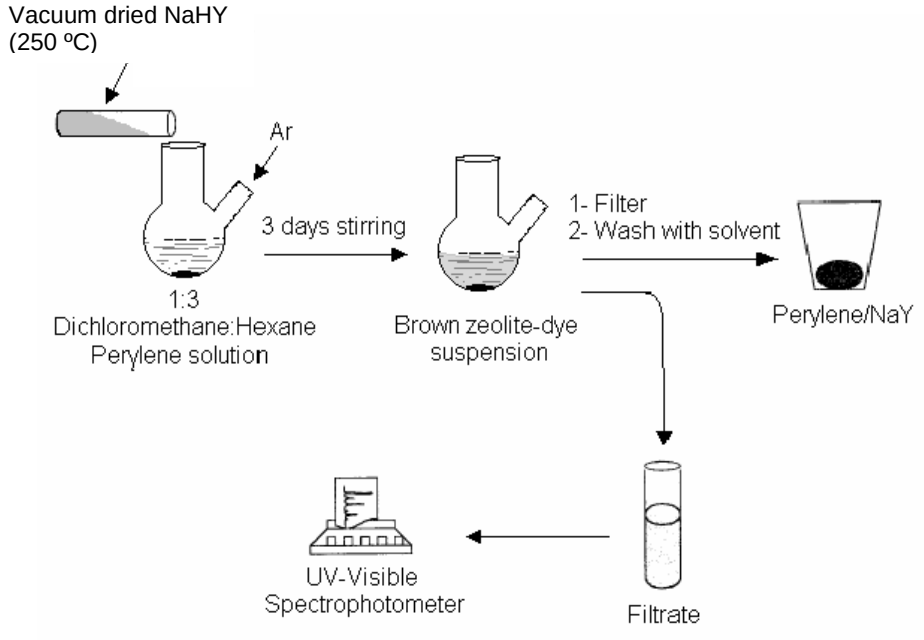

Figure 4.1. Outline of Preparation of Perylene Loaded NaHY

4.1.9.1. UV-Visible Spectroscopy Analysis

UV-Visible spectroscopy analysis was done by Cary 50 Varian Spectrophotometer. Zeolite spectra of solids were taken with oval quartz cells. First the cells were covered with tetradecane and then zeolite samples were placed between these cells. For quantitative analysis, a calibration graph was prepared using standard solutions of perylene at its max. absorbance wavelength (385, 408 and 435 nm). (Figure 4.2, 4.3) Perylene amount of filtrates was calculated from calibration graph and the loading level to NaHY determined.

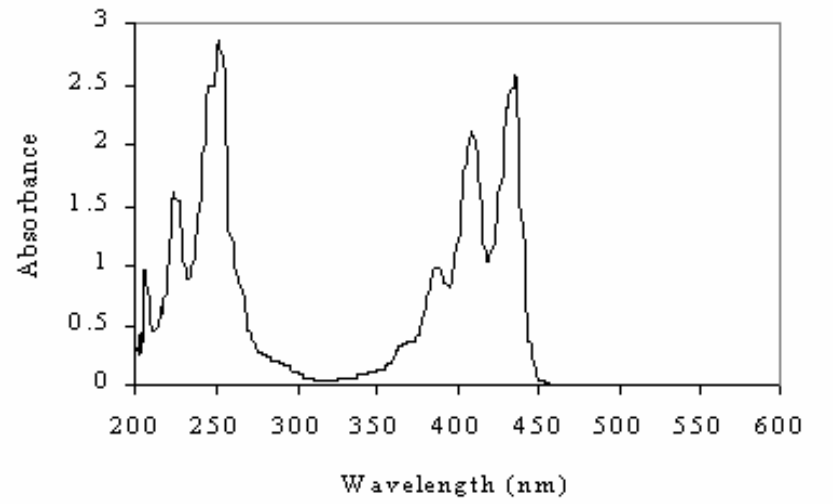

Figure 4.2. UV Spectrum of Perylene in 1:3 DCM:Hexane Solution with the Three Maxima Wavelengths 385, 408 and 435 nm.

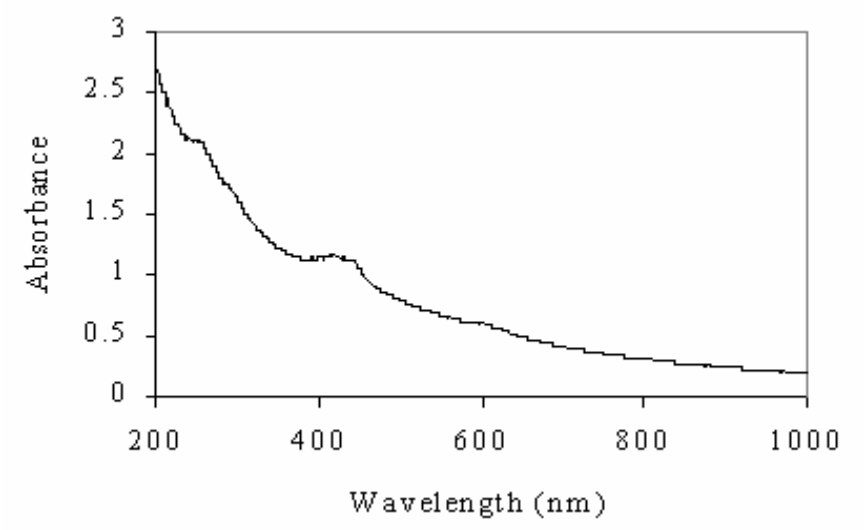

Figure 4.3. UV Spectrum of Perylene Loaded NaHY with the Characteristic Peaks of Perylene at About 408-435 nm.

4.1.10. Preparation of Pyridine Neutralized NaHY

Two different amounts of pyridine were used to neutralize NaHY. In the first one 0.9 mg, and in the second 10.3 mg pyridine was used. In both process, pyridine was added in hexane solution to vacuum dried 300 mg NaHY and stirred for 5 h under Ar atmosphere for diffusion of base molecules into the cages of zeolite. After neutralization procedure, immediately terpene solution was added to pyridine/NaHY and a standard reaction started.

4.1.11. Preparation of Na_2CO_3 neutralized NaHY

Na_2CO_3 was used for the neutralization of acid sites in NaHY. Na_2CO_3/NaHY was prepared by NaHY stirring with 20 % Na_2CO_3 solution under reflux over 24 h. The zeolite suspension was filtered, washed thoroughly by ultra pure water and it was dried at 120 °C.

Other catalysts; Montmorillonite KSF was used as received from Fluka (69867). Synthesized MCM-41 [61] and amorphous silica according to literature was used.

4.2. INTRAZEOLITE REACTIONS

4.2.1. Dehydrogenation Reactions

Dehydrogenation reactions of terpinenes were carried out in a test tube that tightly closed with a suba seal. Zeolite was dried in that tube overnight at 150 °C in an oil bath, under vacuum. A syringe needle that connected to a vacuum pump with a hose was inserted to suba seal for supplying vacuum in drying process. After drying, Ar gas inlet was supplied with another syringe needle that prevents zeolite to contact with air. Terpene solution in hexane was added to the reaction vessel with a syringe. Hexane was dried with metallic Na and degassed with Ar.

Schematic representation of the reaction procedure is shown in Figure 4.4. In a representative example, 20 mg of α-terpinene (Aldrich, 85 %) and internal standard decane dissolved in 8 mL of dry and degassed hexane was added to 300 mg of dry

NaHY. After 15 min of stirring under argon in the dark, zeolite suspension was centrifuged. Hexane solution was separated from zeolite and the zeolite residue stirred with 5 mL portions of THF three times than centrifuged. Hexane solution and THF extracts were collected in the same vessel and analyzed by GC and GC/MS.

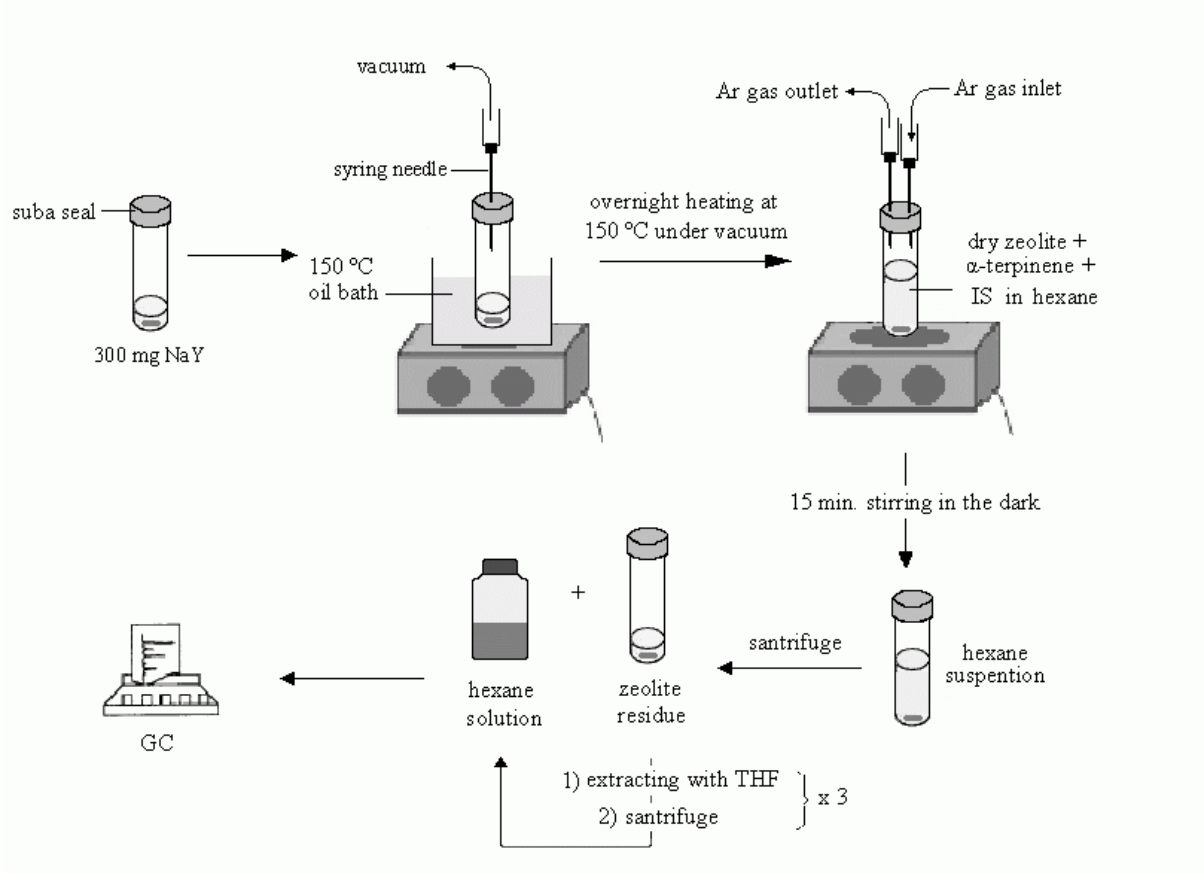

Figure 4.4. Outline of the Terpene Dehydrogenation Procedure

This reaction was done with other zeolites LiHY, KHY, CaHY, CsHY, LiNaHY, CaNaHY, KNaHY, HY, pyridine/NaHY, perylene/NaHY, NaX, CsNaX, NaHβ, NaHMOR and siliceous MCM-41, an acidic clay Montmorillonite KSF and Mesoporous Silica in the same manner. In all the reactions, 300 mg catalyst was used.

4.2.2 Photodehydrogenation and Photooxidation Reactions

Photodehydrogenation and photooxidation reactions were carried out in a cylindrical pyrex photoreactor with inner water-cooling apparatus and the Philips-son-T plus-400W sodium lamp system. Dried and degassed hexane solution of α-terpinene was added to the zeolite containing photoreactor under dry molecular O_2 or Ar atmosphere. After 15 min stirring in photoreactor, zeolite suspension was centrifuged and zeolite residue extracted with THF. Products were determined in the final solution by GC and GC/MS analysis. Tetradecane was used as internal standard. These reactions were done within NaHY and perylene/NaHY. A representative intrazeolite photoreaction was summarized in the Figure 4.5.

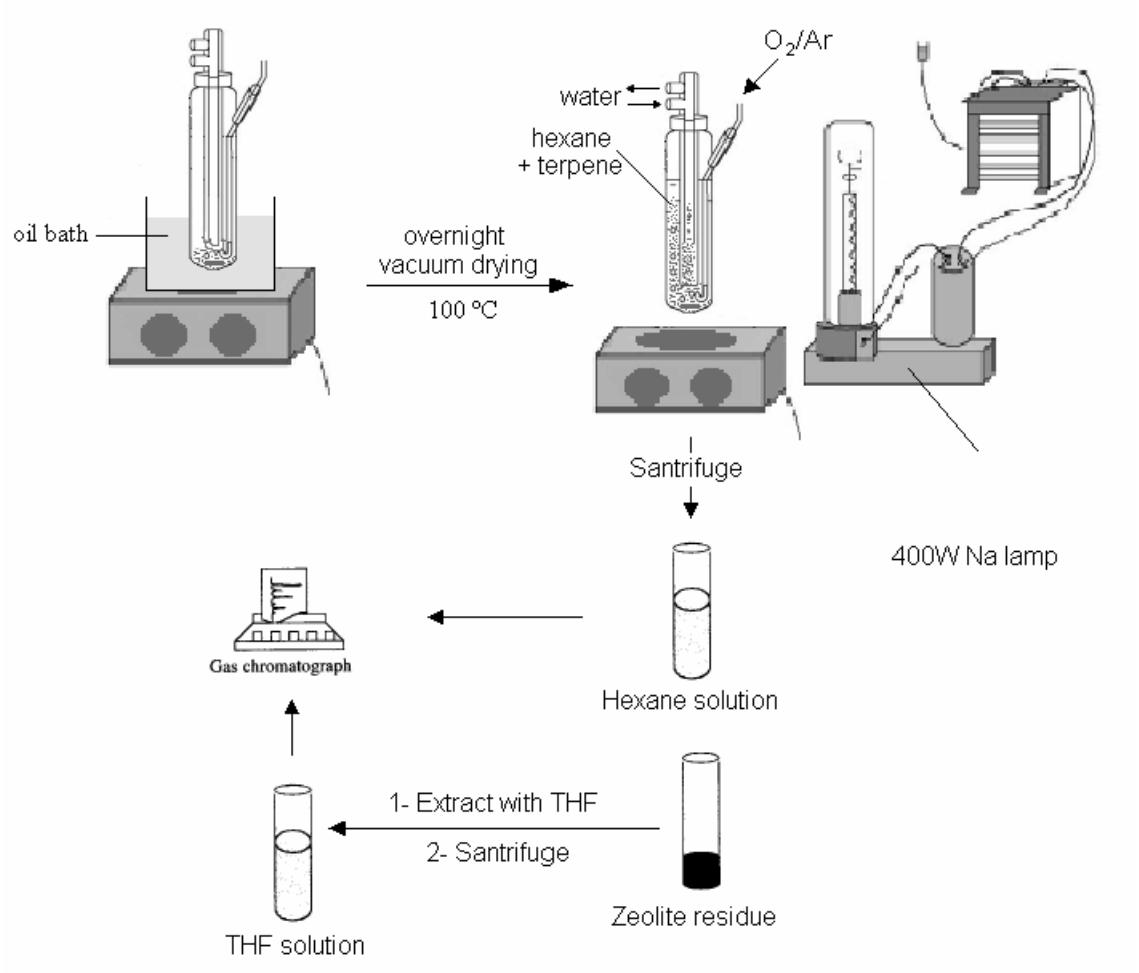

Figure 4.5. Outline of the Intrazeolite Photoreaction

4.2.3. Homogeneous Photooxidation Reactions

Homogeneous system photooxidation reactions were carried out in a cylindrical pyrex photoreactor and 400W sodium lamp as in the intrazeolite reactions. Hexane solution of perylene and α-terpinene was irradiated in the photoreactor under sodium lamp and dry molecular O_2 atmosphere. Products were determined in the final solution by GC and GC/MS analysis (Figure 4.6.). Tetradecane was used as internal standard.

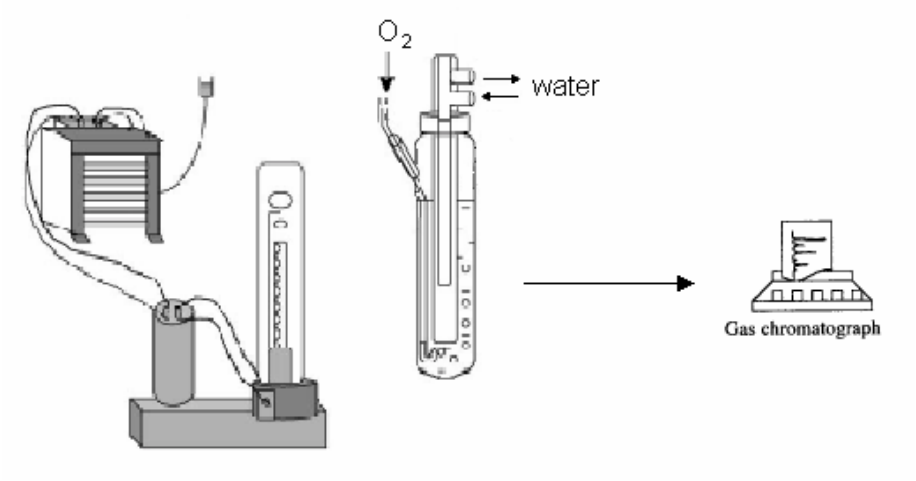

Figure 4.6. Outline of the Homogeneous System Photooxidation

4.3. GC METHOD

The samples were analyzed by GC (Shimadzu GC-17A on a 30 m capillary column and with a FID detector) and GC/MS (Varian Star 3400CX/Varian Saturn 2000, DB5, 30 m, 0.25 mm colomn). The GC and GC/MS programs applied throughout the analysis was as follows: the column temperature was 50 ºC at the beginning of the program and it was heated with a rate of 8 ºC/min up to 100 ºC, then it was heated with a rate of 2 ºC/min up to120 ºC and then it was heated with a rate of 6 ºC/min up to 250 ºC. Throughout the analysis the injector and detector temperatures were kept constant at 280 ºC and 300 ºC, respectively. The analysis was performed on splitless mode. A sample gas chromatogram of the reactant and reaction products according to this temperature program is given in Figure 4.7. The gas chromatogram and the mass spectra

of some dehydrogenation and isomerization products are given in Figure 4.8, Figure 4.9. and Figure 4.10.

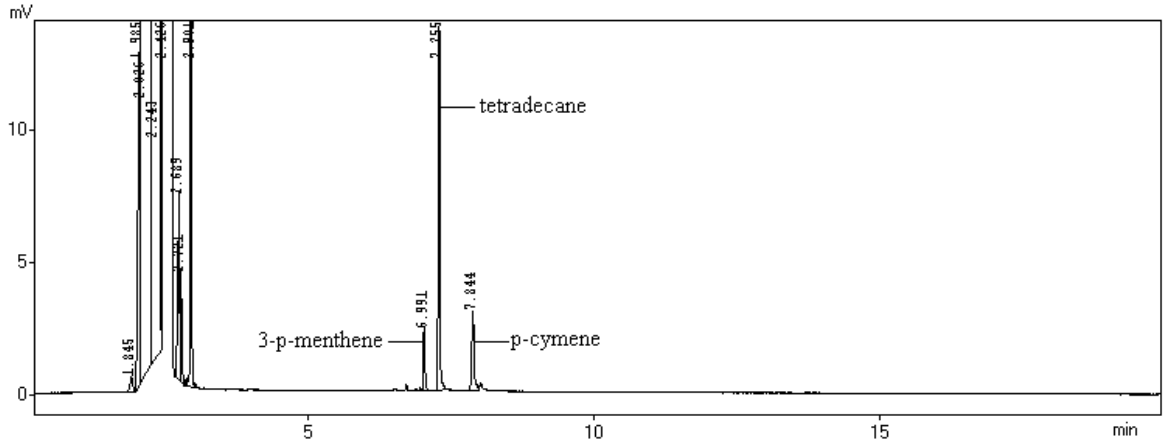

Figure 4.7. Gas Chromatogram of a Reaction Product

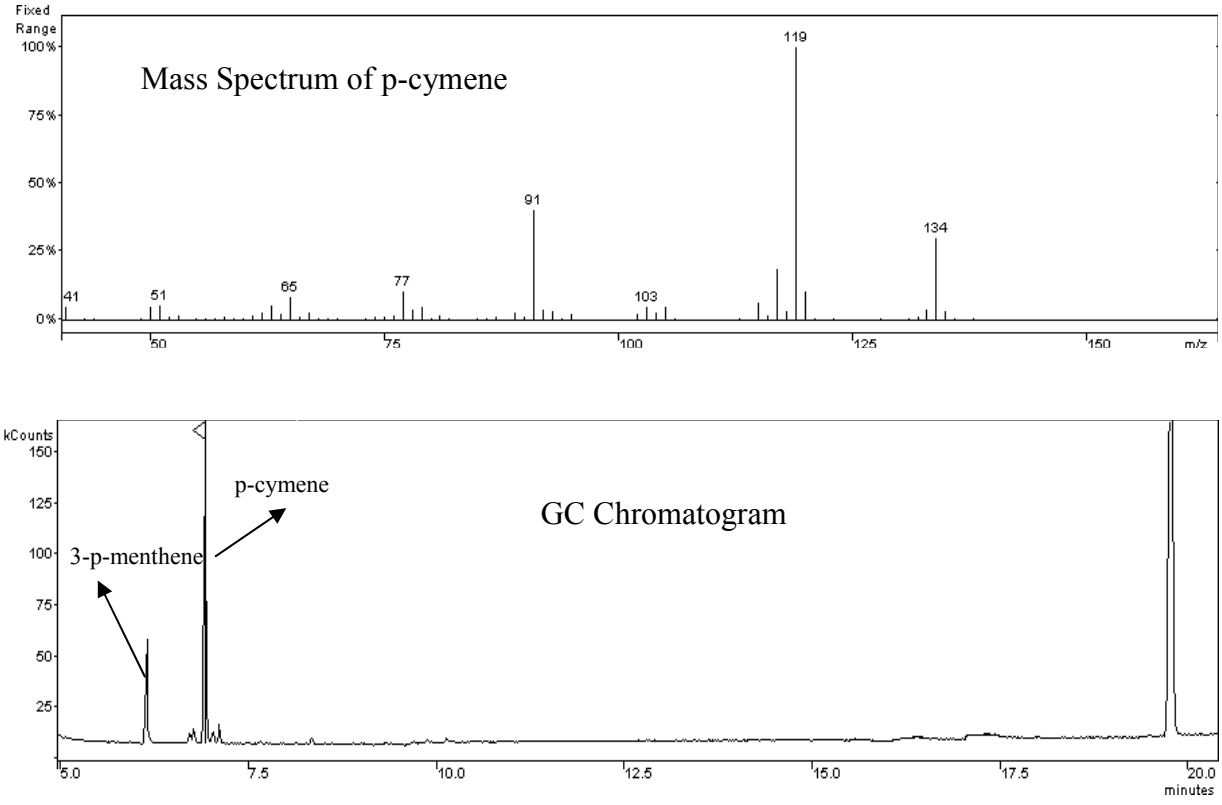

Figure 4.8.GC/MS Chromatogram of p-cymene

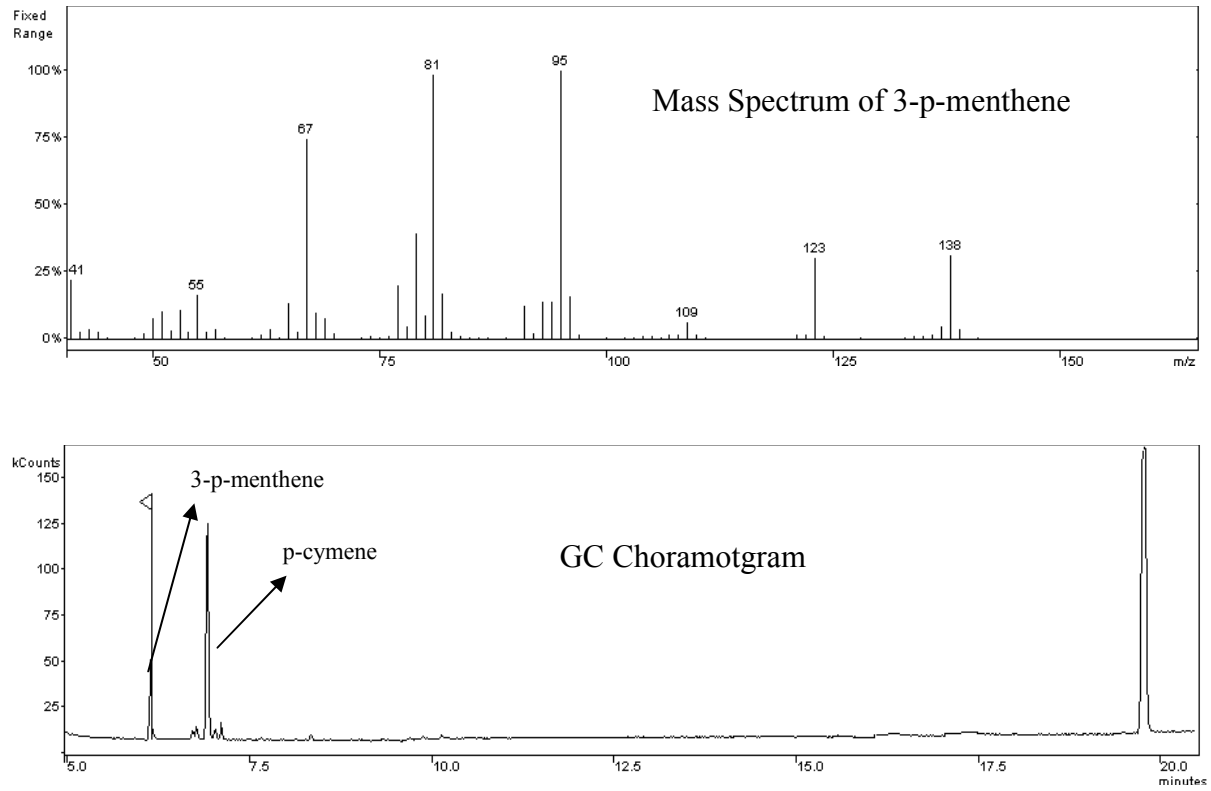

Figure 4.9. GC/MS Chromatogram of 3-p-menthene

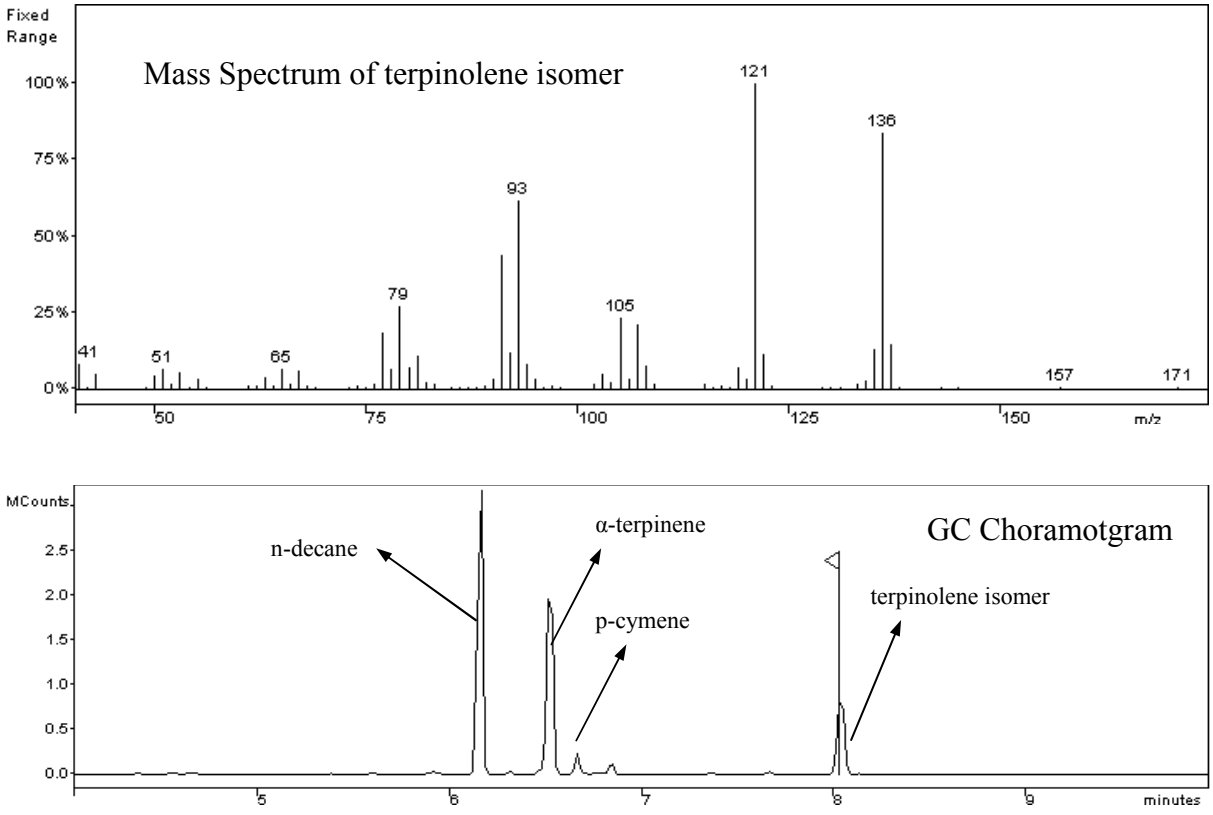

Figure 4.10. GC/MS Chromatogram of terpinolene isomer

4.3.1 Calculation of Reactant and Product Amount on GC

The response factor of reactant and products for the set temperature program of GC was determined for the calculation of amount of reactants and products. As internal standard, decane, dodecane and tetradecane were used. The amount of internal standard does not change throughout the reaction, so the response factor of each compound was determined according to the amounts and areas under the peaks of internal standard and standard compound of interest. A known amount of standard compound with a known amount of internal standard dissolved in the reaction solvent and injected to GC for the determination of response factor of the compound. Only the α-terpinene and p-cymene were available as the standard compound, the response factor of the 3-p-menthene was assumed to be identical to that of α-terpinene. After the analysis was completed according to the set temperature program, the Equation 4.1 and 4.2 are used for the determination of the response factor of that compound:

$$\text{R. F.} = \left(\frac{\text{int. std. area}}{\text{compound area}} \right) \text{x} \left(\frac{\text{compound amount}}{\text{int. std. amount}} \right) \qquad 4.1$$

$$\text{amount of compound} = \left(\frac{\text{int. std. amount}}{\text{int. std. area}} \right) \text{x R. F. x compound area} \qquad 4.2$$

GC chromatogram of a RF standard for the α-terpinene can be seen in the Figure 4.10

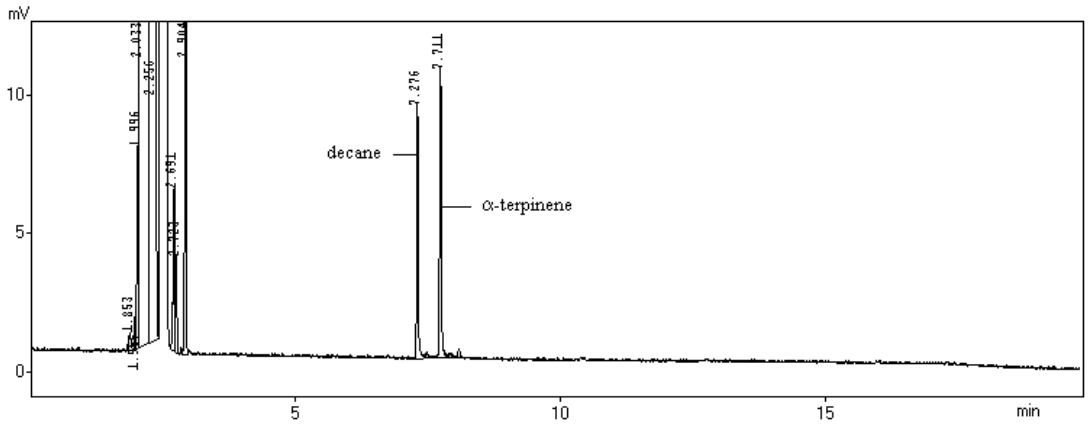

Figure 4.11. GC Chromatogram of a RF Standard for the α-terpinene

CHAPTER 5

RESULTS AND DISCUSSION

For the investigation of dehydrogenation reactions of terpenes, cation-exchanged zeolite-Y, particularly NaHY was used under water free Ar atmosphere and O_2. Photodehydrogenation and photooxidation reactions within NaHY and Perylene/NaHY were carried out for the investigation of photobehavior of catalyst. Some other types of porous materials (X, β, MOR, MCM-41, an acidic clay Montmorillonite KSF and Silica) were used in the control reactions. In order to compare difference in the number of the acid sites between NaHY and NaY pyridine and Na_2CO_3 neutralized NaHY was used.

5.1. DEYHDROGENATIN REACTIONS OF α-TERPINENE WITHIN ZEOLITES

In the dehydrogenation reaction of α-terpinene to p-cymene, 3-p-menthene was also produced as a partial hydrogenation product (Figure 5.1.). This reaction is also called as a partial disproportionation reaction. Product distribution changed according to several parameters. These can be summarized as; type of the exchanged cation, catalyst type, the acidic properties of the type of the catalyst, amount of the reactant, applied irradiation and reaction atmosphere.

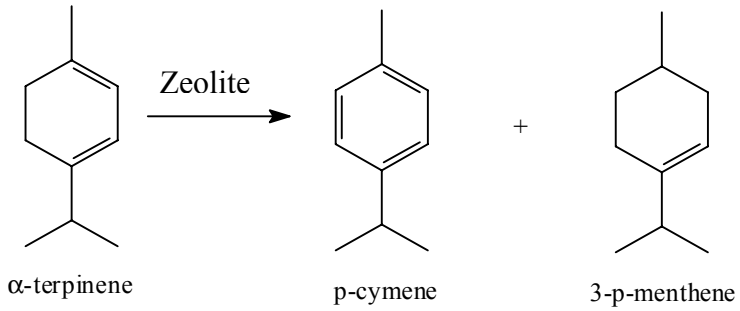

Figure 5.1. Disproportionation of α-terpinene in Zeolites

5.1.1. Effect of Catalyst and Cation Type

Table 5.1. SiO_2/Al_2O_3 Ratio of the Zeolites

Zeolite Type	SiO_2/Al_2O_3 Ratio
NaX	3
NaY	5
NaMOR	20
Naβ	25

As explained in chapter 2, there are two types of acidity on zeolites based on the Brønsted and Lewis acid sites. If the acid site is of Brønsted type, it acts as a proton donor. If the acid site is of Lewis type, it acts as an electron acceptor. The base strength decreases and the electron-accepting ability increases with increasing SiO_2/Al_2O_3. SiO_2/Al_2O_3 ratio of the zeolites used in this study is shown in Table 5.1.

Table 5.2. Effect of the Type of the Catalyst[a]

Entry	Type of Zeolite	α-terpinene left %	3-p-menthene produced %	p-cymene produced %	p-cymene / 3-p-menthene	terpinolene[c] produced %	unknown product %	γ-terpinene produced %	Recovery %
1	NaHY	0	20.0	33.4	1.7	-	-	-	53.4
2	NaY	95.4	-	3.6	-	-	-	-	99.0
3	NaX	92.3	-	4	-	-	-	-	96.3
4	NaCsX	95.0	-	2.8	-	-	-	-	97.8
5	NaHβ	66.7	-	5.2	-	11.3	-	1.9	85.1
6	NaHMOR	90.5	-	3.9	-	-	-	-	94.4
7	MCM-41	82.5	-	4.8	-	9.2	-	-	96.4
8	Amorphous silica	93.1	-	5.3	-	-	-	-	98.4
9[b]	Montmorillonite KSF	52.2	-	5.9	-	-	18.2	-	76.3[d]

[a] Used α -terpinene contains 3-4 % p-cymene, Reaction conditions: 20 mg α-terpinene, 300 mg catalyst vacuum dried at 150 ºC, under Ar atmosphere, 15 min. at RT

[b] 10 mg α-terpinene was used [c] One of the two terpinolene isomer

[d] Recovery is calculated based on weight percent since an unknown product is observed

When we look at the results of dehydrogenation of α-terpinene with different catalysts (Table 5.2.), only remarkable conversion was obtained in the NaHY. NaHY, prepared from NH_4Y, has unexchanged NH_4^+, determined by EDX analysis, in its framework that makes this zeolite more acidic than NaY.

Energy dispersive X-Ray analysis of NaY, NaHY and NH_4Y samples, that allows analysis of elements from Boron up with a detection limit of 0.02-0.05% [62], were done in order to compare the Na content and the ion exchange status of the NaHY with NaY and NH_4Y. Average of five different EDX analysis for each sample was used in the results. The results show us the Na content of the NaHY approximately five times higher than NH_4Y. That shows us ammonium cations in the NH_4Y are exchanged with Na^+. When we compare the Na content of NaY with NaHY, it is still higher than NaHY (Table 5.3.) and this result proves the ion exchange not fully completed and there are still unexchanged NH_4^+ sites that generates Brønsted acidic H^+ sites by thermally on NaHY.

Table 5.3. EDX Results of the Percent Atomic Contents of NaY, NaHY and NH_4Y, Vacuum Dried at 150 ºC

Element	NaY [a] (At %)	NaHY [b] (At %)	NH_4Y [c] (At %)
C	8.0	9.5	6.2
N	4.1	4.5	5.7
O	49.8	51.3	52.9
Na	8.2	3.8	0.7
Al	8.4	8.5	9.4
Si	21.5	22.3	25.2
SiO_2/Al_2O_3	5.1	5.2	5.3

[a] Zeolyst CSV100 SiO_2 / Al_2O_3 =5,1

[b] Exchanged from Zeolyst [c] CSV500 SiO_2 / Al_2O_3 =5,2

Generally the catalytic activity of the zeolites stems from the Brønsted rather than the Lewis acid sites. Lewis acid sites might enhance the strength of nearby Brønsted sites, thereby exerting an indirect influence on the catalytic activity [32]. In the acid catalyzed skeletal isomerization of monoterpenes within porous materials, p-menthadiens, such as α-terpinene, can be disproportionated by Brønsted acid catalysis

into p-menthenes and p-cymene [53]. However, p-cymene can possibly be formed by direct dehydrogenation of α-terpinene with the participation of Lewis acid sites [53]. When we look at the Table 5.2, only formation of disproportionation product 3-p-menthene was observed in NaHY (entry 1), in spite of there are some other Brønsted acids such as natural acidic clay Montmorillonite KSF [63] which made from two silica tetrahedra and an alumina octahedra [64], NaHβ and NaHMOR gave almost no conversion to p-cymene (entries 5, 6 and 9 in Table 5.2.) However, it is seen that in Montmorillonite, there are another reaction pathway to form a different product, which can be thought that a skeletal isomerization product according to literature [53, 60]. In the NaHβ, Brønsted acid catalyzed isomerization of α-terpinene was also observed (Figure 5.2.) to form γ-terpinene and terpinolene or isoterpinolene. Unfortunately, since they have identical retention times in GC, terpinolene and isoterpinolene cannot be differentiated. But according to literature, isoterpinolene appears only after terpinolene [66].

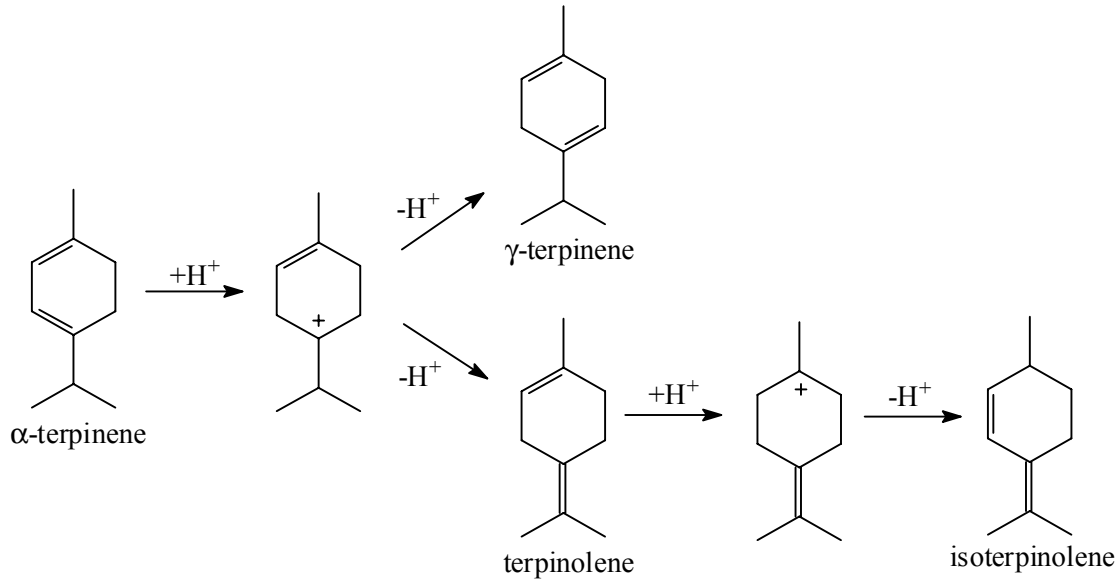

Figure 5.2. Acid catalyzed isomerization of α-terpinene

It was stated that the Brønsted acid sites are responsible for the formation of the protonated species, and the Lewis acid sites, associated nonframework Al atoms, for the formation of cation radicals in zeolites [65]. Disproportionation reaction of monoterpenes occurs by hydride transfer from a neutral monoterpene molecule to the carbocation generated by addition of a proton to another monoterpene molecule [60, 66] (Figure 5.3.).

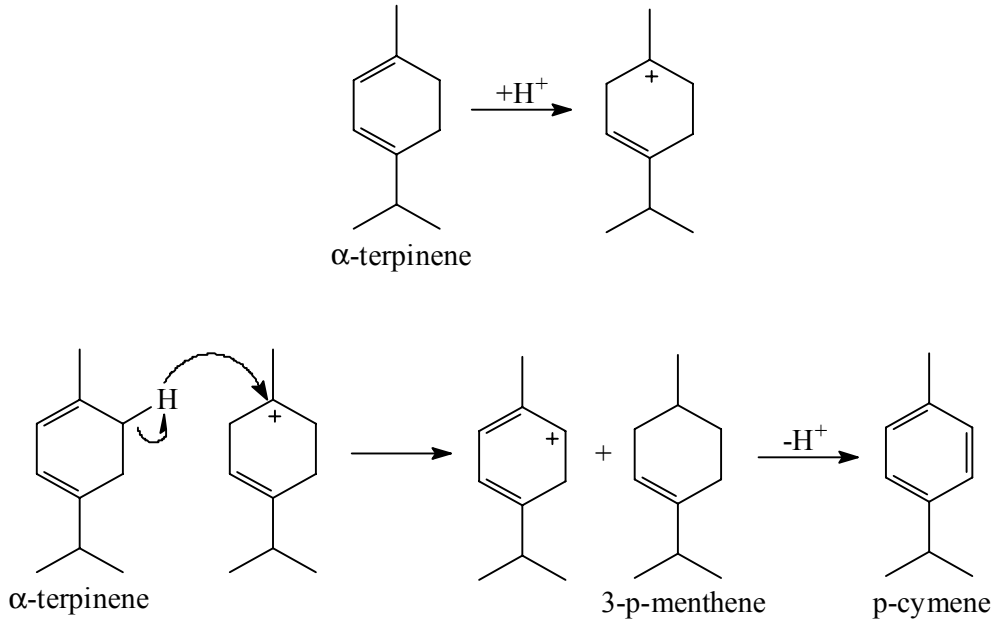

Figure 5.3. Disproportionation mechanism of α-terpinene

As known, bi-molecular disproportionation reactions require more space, due to the bulky intermediates involved, and should be favoured by a high active-site density and restricted by the dimensions of pores and channels of microporous zeolites [53]. That should be the main reason of the no formation of the disproportionation products in other Brønsted acid zeolites, which are NaHβ and NaHMOR with vacant spaces lower than NaHY (entries 5-6) that have Brønsted acid sites results from unexchanged NH_4^+ as in the NaHY.

On the other hand, if this reaction had totally disproportionation, ratio of p-cymene / 3-p-menthene would be 1:1. But the ratio of p-cymene / 3-p-menthene was higher than 1 and it shows p-cymene is also formed by an alternative pathway that should be the direct dehydrogenation of α-terpinene with the participation of Lewis acid sites.

Gutjahr et al. [67] stated that in the zeolite Y pores electronegativity of the cations Li^+, Na^+, Ca^+, K^+ and Cs^+ is much more higher and acts in zeolite cages as electron acceptor as well as a Lewis acid. But protonated form of a zeolite does not show Lewis acidity unless it is activated at 400 ºC [67]. Also it was indicated that electron holes are generated thermally on the zeolite Y lattice [19, 25, 60] and these

have highly positive redox potential and these holes cause the electron abstraction from guest molecules as a Lewis acid. In this study, it can be seen that the generation of electron holes occurs at lower temperatures such as 150 ºC.

In the direct dehydrogenation of α-terpinene, Lewis acid sites abstract an electron with single electron transfer from guest molecule to form radical cation and then radical cation expels a proton to form an allylic radical. In the last step, a hydrogen atom is lost forming p-cymene.

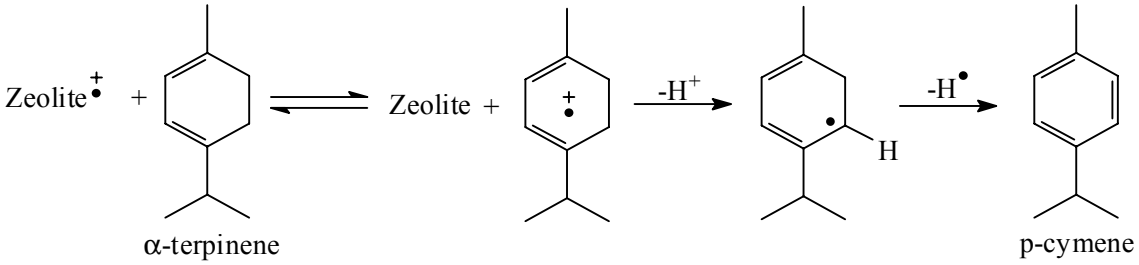

Figure 5.4. Lewis acid catalyzed dehydrogenation of α-terpinen

In the experiments with mesoporous structured zeolite MCM-41 [59] and amorphous silica (entries 7-8), which have no Al in their structure, no conversion to p-cymene was observed. In the MCM-41, isomerization product one of the two terpinolene isomer was also observed. NaX was inert in the dehydrogenation reaction as expected, because it has higher Al content than NaY, so it is less acidic.

Table 5.4. Effect of the Cation Type[a]

Entry	Zeolite	α-terpinene left %	p-cymene produced %	3-p-menthene produced %	p-cymene / 3-p-menthene	terpinolene[e] produced %	Recovery %
10	NaHY	0	33.4	20.0	1.7	-	53.4
11	NaY	95.4	3.6	-	-	-	99.0
12[b,e]	Calcined NaHY	0	39.0	9.2	4.2	-	48.2
13[e]	Calcined NaY	59.1	5.0	-	-	23.7	87.8
14[c]	CaHY	0	38.3	15.2	2.5	-	53.5
15	CaNaHY	0	26.5	8.0	3.3	-	34.5
16[c]	LiHY	0.5	39.6	16.8	2.4	-	57.0
17	LiNaHY	6.1	29.4	11.4	2.6	1.6	48.2
18[d,e]	HY	1.2	14.5	7.0	2.1	-	22.7
19[c]	KHY	40.0	21.4	3.3	6.5	7.8	72.5
20	KNaHY	59.4	11.9	3.1	3.8	4.4	78.8
21[c]	CsHY	72.2	10.9	-	-	-	83.1

[a] Used α-terpinene contains 3-4 % p-cymene, Reaction conditions: 20 mg α-terpinene, 300mg catalyst vacuum dried at 150 ºC, under Ar atmosphere, at RT [b] 10 mg α-terpinene, [c] 5 mg α-terpinene, [d] 50 mg α-terpinene was used [e] calcined at 550 ºC for 10 h [e] One of the two terpinolene isomer

When we compare the results of NaHY and calcined NaHY according to their ratio of p-cymene / 3-p-menthene, it can be shown that disproportionation ratio increases with calcination of NaHY, which causes the formation of Lewis acid sites, and reaction undergoes the direct dehydrogenation pathway.

As shown in Table 5.2. and 5.4. among all catalysts of only over Na^+, Ca^+, and Li^+ exchanged zeolite Y, calcined NaHY and HY, α-terpinene conversion was almost complete. In these zeolites ratio of p-cymene / 3-p-menthene is the lowest and disproportionation and direct dehydrogenation are competitive.

In the double cation exchanged zeolites, because of extra cation exchange process, there are less unexchanged NH_4^+ that lowers the acidity of the zeolites so the conversion is lower and direct dehydrogenation rate is higher than the single cation exchanged ones (entries 15, 17 and 20).

Spontaneous formation of radical cations within CaY and NaY are described before in the literature [27, 68]. In the fist one, electron transfer formation of the corresponding radical cation of 1,5-dithiacyclooctane was observed in CaY which is known as acidic, with a color formation that wasn't observed in the solution [68]. In the second example, α-terpinene dehydrogenated to p-cymene with a spontaneous electron transfer formation of the radical cation occurs by the help of an electron deficient sentisizer MV^{2+}, which loaded previously into the NaY cages [27]. In the absence of this sentisizer no formation of products was observed as in this study. NaY has much less acid sites as compared to CaY [44]. When we use NaHY, α-terpinene was totally consumed to form p-cymene and 3-p-menthene. This shows us the acidic sites of the NaHY are higher than the NaY.

As soon as we added α-terpinene to zeolite, which able to form p-cymene, the orange color formation was started to occur and after 15 min. an intense orange color was observed on the zeolite while solution remained colorless. In order to investigate the source of the color we added concentrated hexane solution of α-terpinene and p-cymene onto NaHY, vacuum dried at 150 ºC, then zeolite was centrifuged and separated from solution. After this process, α-terpinene added zeolite showed dense orange color and p-cymene added zeolite was slightly beige to white color. When we compare the UV-Visible spectrum of these zeolites respectively, in the first one, three main peaks at 250-300, 405 and 502 nm are shown while the other has only the p-cymene peak (Figure 5.5.). Formation of peaks not observed in solution that have longer wavelengths shows us a formation of different product, which was thought the radical cation of corresponding molecule, as in the other examples [44, 68, 69].

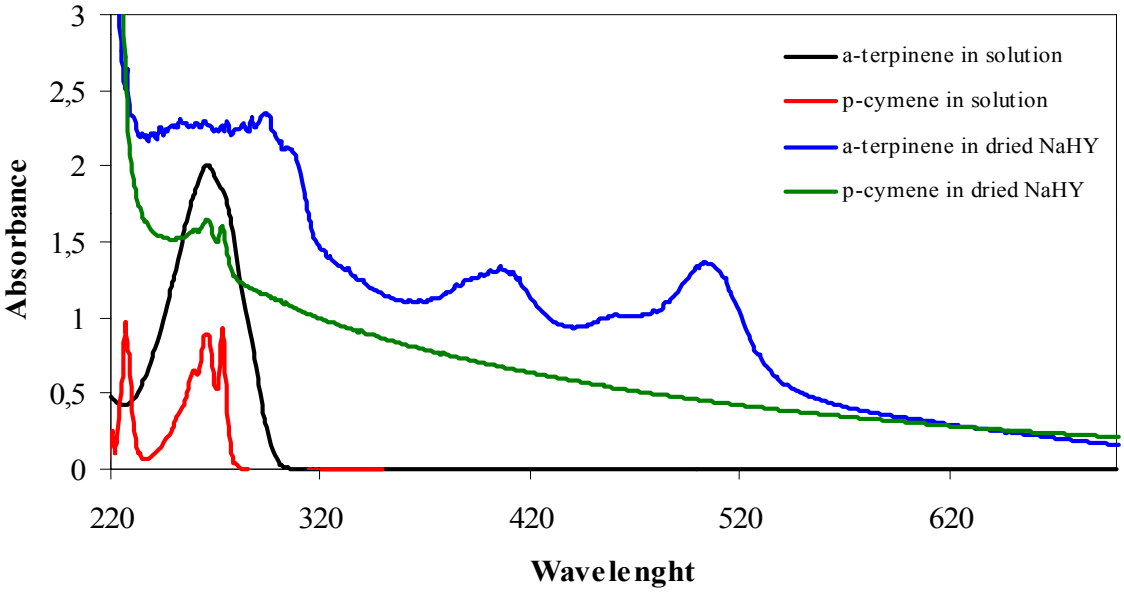

Figure 5.5. UV-Visible spectra of α-terpinene and p-cymene in dried NaHY, and freshly prepared hexane solutions of α-terpinene and p-cymene.

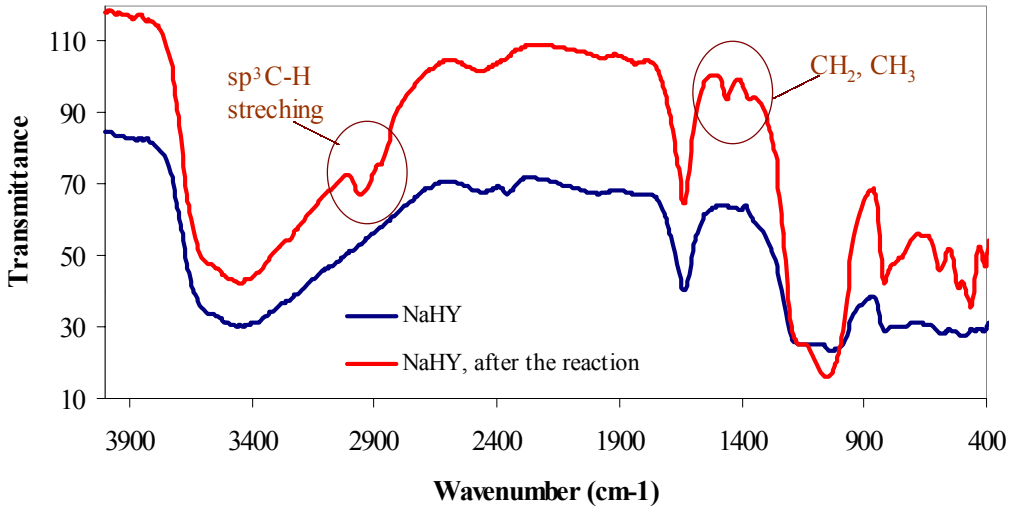

Figure 5.6. FTIR spectra of NaHY and after reaction with α-terpinene in dried NaHY

After with a 100 mg a-terpinene reaction and then extraction with THF, FTIR spectrum of zeolite was taken (Figure 5.6.). FTIR spectrum of NaHY, after the reaction, confirms the existence of an organic compound in zeolite but it is not enough to identify this molecule.

On the other hand in dried or calcined NaY, there was no such colored indication (Figure 5.7.).

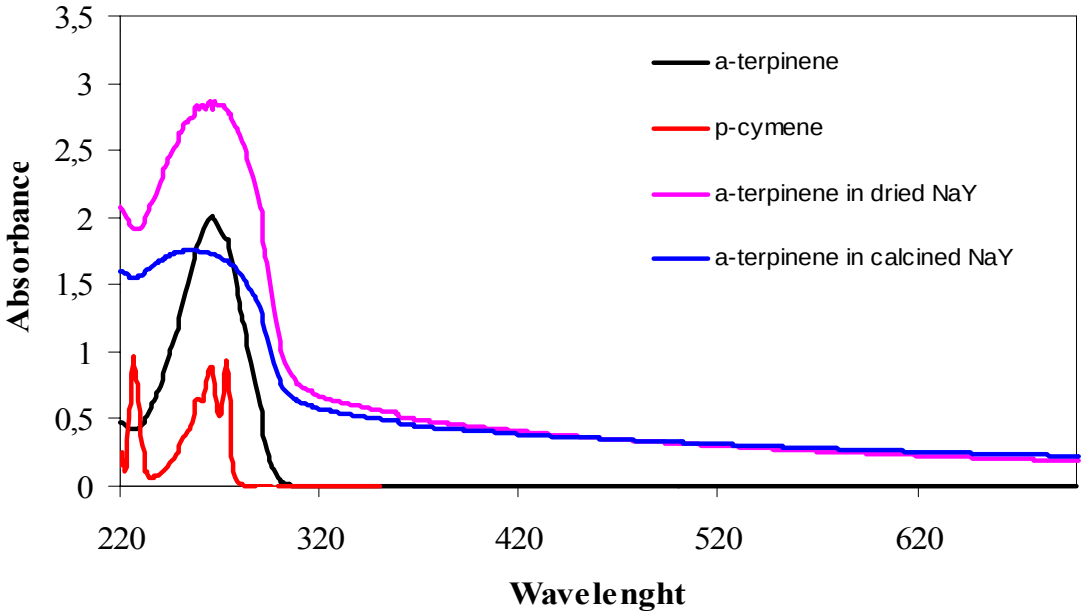

Figure 5.7. UV-Visible spectra of α-terpinene in dried and calcined NaY, and freshly prepared hexane solutions of α-terpinene and p-cymene.

Among the cation exchanged Y zeolites K^+ and Cs^+ gave less conversion. It is well known that as the radius of the cation increases the basic character of the zeolite increases. When we look at the results (entries 19-21) in Table 5.3, increasing basicity of the zeolites verify the decrease of the conversion. Also the ratio of p-cymene / 3-p-menthene are the highest values with these zeolites indicating that the Lewis acid sites are more dominating within these zeolites and it can be said that these sites are not enough to high conversion. Cs has quite basic character that makes zeolite basic and also lowers the pore size of zeolite that may prevent the diffusion of most of the guest molecules into the zeolite.

5.1.2. Effect of Drying

Table 5.5. Effect of Drying[a]

Entry	Conditions of Zeolite and Solvent	α-terpinene left %	p-cymene produced %	3-p-menthene produced %	p-cymene / 3-p-menthene	Recovery %
22	NaHY	0	33.4	20.0	1.7	53.4
23[b]	Non vacuumed NaHY	98.5	1.5	-	-	100
24[c]	Non dried NaHY	98.0	2.0	-	-	100
25	NaHY, with not freshly-dried Hexane	71.0	9.8	3.5	2.8	84.3

[a] Used α-terpinene contains 3-4 % p-cymene, Reaction conditions: 20 mg α-terpinene, 300mg catalyst vacuum dried at 150 ºC, 15 min. at RT , solvent: freshly dried and degassed hexane [b] dried at 150 ºC
[c] Zeolite used without drying.

When zeolite used without prior drying or dried without vacuum (entries 23-24 in Table 5.5.), there was no conversion observed. It can be thought that the reason of inactivity it probably due to blocking of Lewis acid sites by water molecules that cannot be removed at 150 ºC without vacuum. According to ratio of p-cymene / 3-p-menthene of entry 25, when the solvent is moistened, most of the Brønsted acid sites seem to be inhibited.

5.1.3. Effect of Reactant Amount

Table 5.6. Effect of the Amount of The Reactant[a]

Entry	Amount of α-terpinene	% α -terpinene left	% p-cymene produced	% 3-p-menthene produced	p-cymene / 3-p-menthene	% Recovery
26	5 mg	0	42.1	15.5	2.7	57.6
27	10 mg	0	29.5	19.1	1.5	48.5
28[b]	10 mg	0	26.4	17.1	1.5	43.5
29	20 mg	0	33.4	20.0	1.7	53.4
30	50 mg	3.7	32.0	18.1	1.8	54.0
31	100 mg	24.2	25.5	11.7	2.2	61.5
32	200 mg	76.9	10.2	3.6	2.8	90.7

[a] Used α-terpinene contains 3-4 % p-cymene, Reaction conditions: 300mg NaHY vacuum dried at 150 ºC, under Ar atmosphere, 15 min. at RT

[b] at 50 ºC

As shown in the Table 5.6, as the amount of the reactant increases while keeping the zeolite amount constant, the consumption of α–terpinene in the reaction decreases up to a limited value. This shows us that the zeolite has a limited adsorption capacity that is in this case between 20-50 mg for a 15 min. reaction and it seems to be 15 min not enough to consume α–terpinene higher amounts than 50 mg.

When we compare the entries 27 and 28, carried out at RT and 50 ºC respectively, there are no considerable difference in conversion.

5.1.4. Effect of the Monoterpene Type

Table 5.7. Effect of Monoterpene[a]

Entry	Reactant	% Amount of reactant left	% p-cymene produced	% 3-p-menthene produced	p-cymene / 3-p-menthene	% α -terpinene produced	% Recovery
33	α-terpinene	0	33.4	20.0	1.7	-	53.4
34	γ-terpinene	66,7	12,6	5,0	2.5	7,1	91,4

[a] Used α-terpinene contains 3-4 %, γ-terpinene 2 % p-cymene, Reaction conditions: 20 mg reactant, 300mg NaHY vacuum dried at 150 ºC, under Ar atmosphere, 15 min.

When we use a different monoterpene, γ-terpinene, that has not conjugated 2 double bonds, it didn't fully convert to p-cymene and 3-p-menthene, and partially isomerized to α-terpinene after a 15 min. reaction. These results shows that the existence of conjugated double bonds facilitate the radical cation formation, which leads to products.

5.1.5. Effect of Irradiation and Sensitizer

Table 5.8. Irradiation and Sensitizer Effect[a]

Entry	Irradiation conditions with NaHY	α-terpinene left %	p-cymene produced %	3-p-menthene produced %	p-cymene / 3-p-menthene	Recovery %
35	Under Ar	0	27.2	9.7	2.8	36.9
36	Under O_2	0	18.0	4.7	3.8	22.7
37	Perylene/NaHY under O_2	0	37.4	1.1	34	38.6

[a] Used α-terpinene contains 3-4 % p-cymene, Reaction conditions: 5 mg α-terpinene, 300mg catalyst vacuum dried at 150 ºC, 15 min., at RT

In the homogeneous system, according to the results, photooxidation of α-terpinene solution with the molecular O_2 and with a photosensitizer (perylene), endoperoxide product of α-terpinene, ascaridole was the major product. Without a photosensitizer, p-cymene is the major product. In literature [13, 14], endoperoxide product, ascaridole is would be the major product when α-terpinene treated in the presence of perylene derivatives as singlet oxygen producer. However, in our case when

the reaction is performed within the zeolite, no singlet oxygen reaction product formed rather the products were p-cymene and 3-p-menthene only. However a striking difference was the much higher p-cymene / 3-p-menthene ratio observed (Table 5.8.).

5.1.6. Effect of the Acidic Properties of the NaHY

a) Effect of Treating NaHY with Pyridine:

Table 5.9. Effect of Treating with Pyridine[a]

Entry	Zeolite	% α-terpinene left	% p-cymene produced	% 3-p-menthene produced	p-cymene / 3-p-menthene	% Recovery
38	NaHY	0	33.4	20.0	1.7	53.4
39	NaY	95.4	3.6	-	-	99.0
40[b,c]	Pyridine/NaHY	7.8	42.3	14.0	3.0	64.1
41[b,d]	Pyridine/NaHY	97.6	7.1	-	-	104.8

[a] Used α-terpinene contains 3-4 % p-cymene, Reaction conditions: 20 mg α-terpinene, 300mg catalyst vacuum dried at 150 ºC, under Ar atmosphere, 15 min.

[b] 5 mg α-terpinene was used [c] 0.94 mg pyridine was used [d] 10.3 mg pyridine was used

According to results, after treating NaHY with 0.94 mg pyridine, it can be shown that there are still acid sites, which catalyze the dehydrogenation reaction. Also p-cymene / 3-p-menthene ratio says that pyridine neutralize predominantly the Brønsted acid sites. After treating NaHY with 10.3 mg pyridine it seems to be all acid sites was neutralized (Table 5.9.).

b) Effect of the Neutralization of Acid Sites of NaHY with Na_2CO_3:

Table 5.10. Effect of Neutralization with Na_2CO_3[a]

Entry	Zeolite	% α-terpinene left	% p-cymene produced	% 3-p-menthene produced	p-cymene / 3-p-menthene	% Recovery
42	NaHY	0	33.4	20.0	1.7	53.4
43	Na_2CO_3/NaHY	90.9	3.4	-	-	94.3
44	NaY	95.4	3.6	-	-	99.0

[a] Used α-terpinene contains 3-4 % p-cymene, Reaction conditions: 20 mg α-terpinene, 300mg catalyst vacuum dried at 150 ºC, under Ar atmosphere, 15 min.

For the neutralization of all the acid sites of NaHY, we did a further ion-exchange with Na_2CO_3. After the neutralization process also no conversion of α-terpinene was observed (entry 43). When we compare the Na content of Na_2CO_3 treated and non-treated NaHY, Na content of modified zeolite almost reached to the NaY. This result shows that exchange with Na_2CO_3 ends up with the exchange of remaining NH_4^+ with Na^+ (Table 5.11.). So, Na_2CO_3/NaHY acts as NaY.

Table 5.11. EDX results of the percent atomic contents of NaY, NaHY and Na_2CO_3/NaHY, vacuum dried at 150 ºC

Element	NaY [a] (At %)	Na_2CO_3 / NaHY [b] (At %)	NaHY [b] (At %)
C	8.0	8.8	9.5
N	4.1	4.3	4.5
O	49.8	50.3	51.3
Na	8.2	7.6	3.8
Al	8.4	7.5	8.5
Si	21.5	21.4	22.3
SiO_2/Al_2O_3	5.1	5.7	5.2

[a] Zeolyst CSV100 SiO_2 / Al_2O_3 =5.1

[b] Exchanged from Zeolyst CSV500 SiO_2 / Al_2O_3 =5.2

5.2. X-RAY DIFFRACTION ANALYSIS

5.2.1. X-Ray Diffraction Analysis of NaY, NaHY and NH_4Y

In order to investigate the effect of cation exchange to the crystalline structure of the zeolite X-Ray analysis of the NaY, NaHY and NH_4Y were done (Figure 5.8.). The results show us that cation exchange has no effect on the crystalline structure.

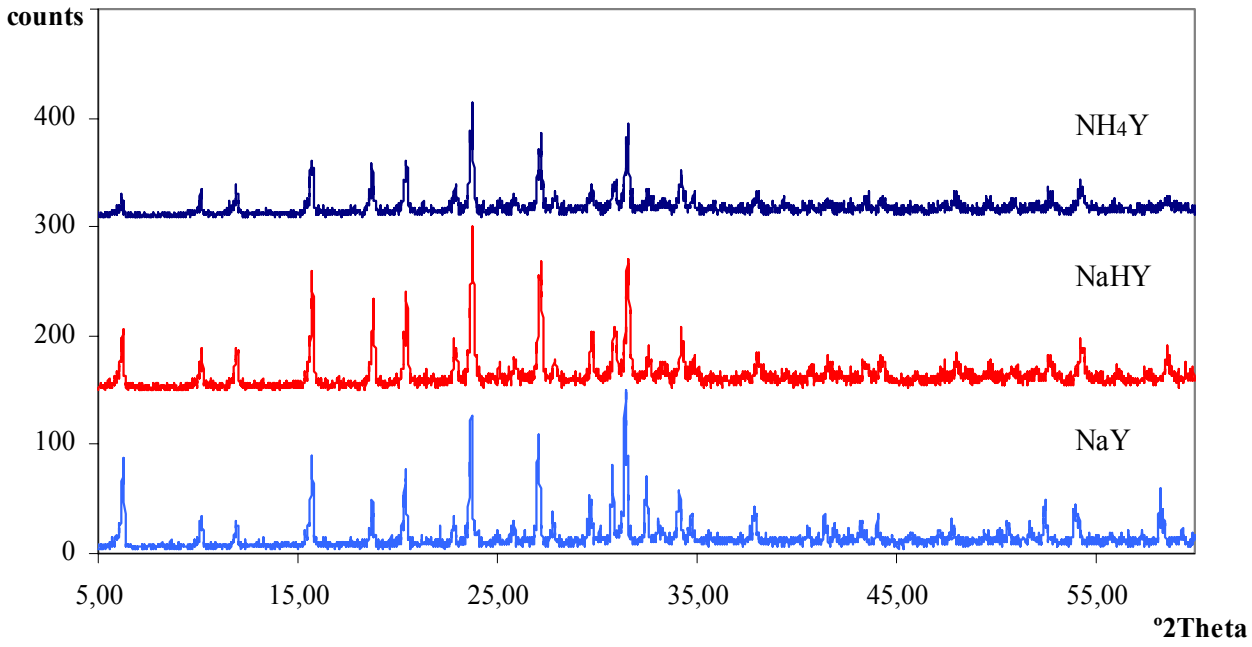

Figure 5.8. XRD patterns of NaY, NaHY and NH_4Y vacuum dried at 150 ºC

5.2.1. X-Ray Diffraction Analysis Of Dried, Non-Dried And Calcined NaHY

In order to investigate the effect of drying and calcination to the crystalline structure of the zeolite X-Ray analysis of the dried, non-dried and calcined NaHY were done (Figure 5.9.). The results show us that also drying conditions has no effect on the crystalline structure.

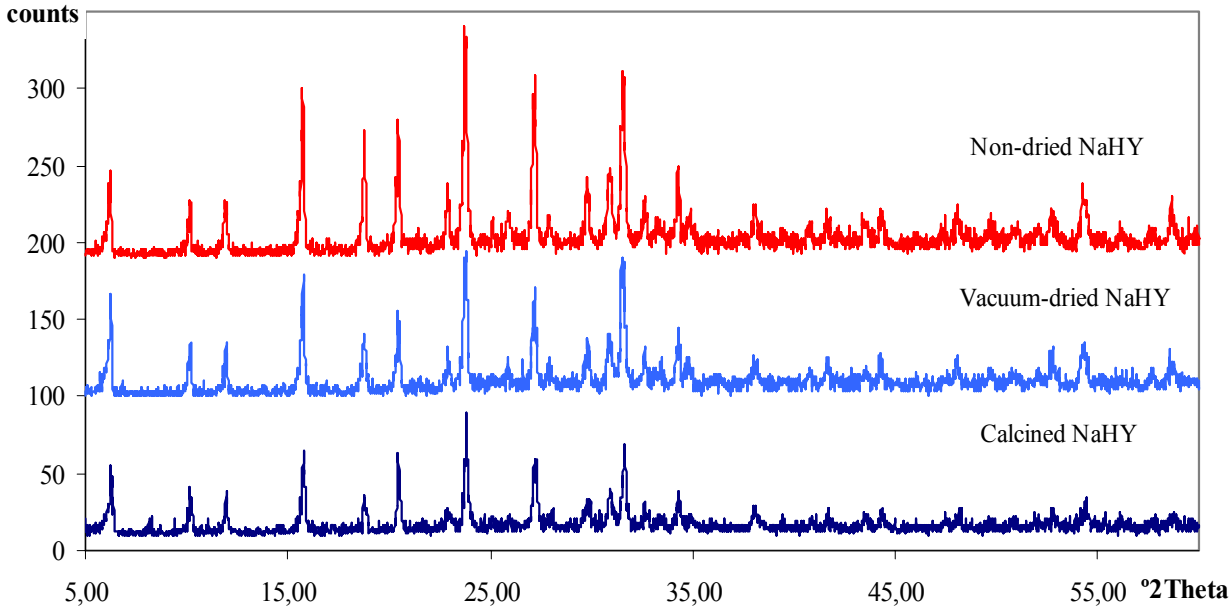

Figure 5.9. XRD patterns of dried, non-dried and calcined NaHY

CHAPTER 6

CONCLUSION

One of the most used monoterpene, α-terpinene, disproportionated by the zeolites which posses both Brønsted acid character into 3-p-menthene and p-cymene.

Brønsted acid catalyzed disproportionation reaction initiated by the carbocation formation inside the zeolites, but in the Lewis acid catalyzed dehydrogenation, reaction initiated with a radical cation formation by a single electron transfer from terpene molecule to the electron holes of zeolite.

p-cymene / 3-p-menthene ratio gave the information about rates of disproportionation and direct dehydrogenation reactions. It was showed that these two reactions competitive according to the cation type and drying conditions.

NaHY and NaY was compared with respect to their catalytic activity and difference in composition. The experiments show that all NH_4^+ did not fully exchange in the in the ion-exchange process with Na^+ and that makes NaHY more acidic than NaY.

Best formation of p-cymene was observed in the NaHY, LiHY and CaHY exchanged from NH_4Y that have relatively small cations, which more acidic than the larger ones.

With the catalysts that have Brønsted sites except ion-exchanged zeolite Y, no conversion or only acid catalyzed isomerization reactions occur that shows the Brønsted acidity was not enough to catalyze the dehydrogenation of α-terpinene. Also Lewis acidic character and the structure morphology are the most important factors affecting the conversion. Lewis acidity is influenced from the cation and zeolite type.

REFERENCES

[1] Hydrogenation and dehydrogenation, (Source: http://www.chemical-industry.org.uk/chemfiles/chemfiles.php3/processes/104).

[2] Ternay A. L.; *Contemporary Organic Chemistry*, (Sounders Comp., 1979.).

[3] Itoh N.; "Dehydrogenation process" *United States Patent* 5 449 848 (12.09.1995), Agency of Industrial Science and Tech.

[4] Liquori A. M., Palazzo A.; "Chemical process and catalyst therefore", *United States Patent* 3 280 207 (18.10.1966), Colgate-Palmolive Corp.

[5] Wideman L. G., Kuczkowski J. A.; "Process for the conversion of terpenes to cymenes" *United States Patent* 4 382 152 (03.05.1983), The Goodyear Tire & Rubber Comp.

[6] Wideman L. G.; "Process for the conversion of terpenes" *United States Patent* 4 375 572 (01.03.1983), The Goodyear Tire & Rubber Comp.

[7] Kirkpatrick W. J.; "Cymene production" *United States Patent* 2 402 898 (25.06.1946), Hercules Powder Comp.

[8] Liquori A. M., Palazzo A.; "Chemical process and catalyst therefore", *United States Patent* 3 312 635 (03.05.1967), Colgate-Palmolive Corp.

[9] Martin R., Gramlich W.; "Preparation of p-cymene and homologous Alkylbenzenes" *United States Patent* 4 720 603 (19.01.1988), BASF AG.

[10] Weyrich P.A., Treviño H., Hoelderich W., Sachtler W. M. H.; "Characterization of Ce promoted, zeolite supported Pd catalysts" *Appl. Catal. A: Gen.* **163**, (1997), 31-44.

[11] Buhl D., Weyrich P.A., Sachtlerb W.M.H., Hölderich W.F.; "Support effects in the Pd catalyzed dehydrogenation of terpene mixtures to p-cymene" *Appl. Catal. A: Gen.* **171**, (1998), 1-11.

[12] Buhl D., Roberge D.M., Hölderich W.F.; "Production of p-cymene from a-limonene over silica supported Pd catalysts" Appl. Catal. A: Gen. **188**, (1999), 287–299.

[13] L. Chen, L.A. Lucia, E.R. Gaillard, H. Icil, S. Icli, D.G. Whitten,; "Photooxidation of a conjugated diene by an exciplex mechanism: Amplification via radical chain reactions in the perylene diimide-photosensitized oxidation of α-terpinene" *J. Phys. Chem. A*, **102**, (1998), 9095-9098.

[14] Alp S., Erten S., Karapire C., Köz B., Doroshenko A. O., Içli S.; "Photoinduced energy–electron transfer studies with naphthalene diimides" *J. Photochem. Photobiol. A: Chem.* **135**, (2000), 103–110.

[15] Yang S., Kondo J. N., Domen K.; "Formation of alkenyl carbenium ions by adsorption of cyclic precursors on zeolites" *Catal. Today*, **73**, (2002), 113–125.

[16] Gener I., Moissette A., Brémard C.; "Electron transfer mechanisms of biphenyl sorption in M-ZSM-5 (M =H^+, Cu^{2+}) zeolites" *Chem. Commun*. (2000), 1563–1564.

[17] Folgado J. V., Garcia H., Marti V., Esplfi M.; "ESR Study of Thianthrenium Radical Cation within Acid Zeolites" *Tetrahedron*, **53**, (1997), 4947-4956.

[18] Chen F. R., Fripiat J. J.; "Free Radicals Formed in the Adsorption of Saturated Hydrocarbons on H-Mordenite" *J. Phys. Chem*. **97**, (1993), 5796-5797.

[19] Yoon, K. B.; "Electron- and charge- transfer reactions within zeolites" *Chem. Rev.* **93**, (1993), 321–339.

[20] Rao V. J., Prevost N., Ramamurthy V., Kojima M., Johnston L. J.; "Generation of stable and persistent carbocations from 4-vinylanisole within zeolites" *Chem. Commun.* (1997), 2209.

[21] Sen S. E., Smith S. M., Sullivan K. A.; "Organic Transformations using Zeolites and Zeotype Materials" *Tetrahedron*, **55**, (1999), 12657-12698.

[22] Stamires D. N., Turkevich J.; "Electron Spin Resonance of Molecules Adsorbed on Synthetic Zeolites" *J. Am. Chem. Soc*. **86**, (1964), 749.

[23] Ramamurthy V., Caspar J. V., Corbin D. R.; "Generation, Entrapment, and Spectroscopic Characterization of Radical Cations of α,ω-Diphenylpolyenes within the Channels of Pentasil Zeolites" *J. Am. Chem. Soc*. **113**, (1991), 594-600.

[24] Yoon K. B., Park Y. S., Kochi J. K.; "Interfacial Electron Transfer to the Zeolite-Encapsulated Methylviologen Acceptor from Various Carbonylmanganate Donors. Shape Selectivity of Cations in Mediating Electron Conduction through the Zeolite Framework" *J. Am. Chem. Soc*. **118**, (1996), 12710-12718.

[25] Park Y. S., Um S. Y., Yoon K. B.; "Charge-Transfer Interaction of Methyl Viologen with Zeolite Framework and Dramatic Blue Shift of Methyl Viologen-Arene Charge-Transfer Band upon Increasing the Size of Alkali Metal Cation" *J. Am. Chem. Soc*. **121**, (1999), 3193-3200.

[26] Ramamurthy V.; "Controlling photochemical reactions via confinement: zeolites" *J. Photochem. Photobiol. C: Photochem. Rev. 1*, (2000), 145–166.

[27] Stratakis, M.; Stavroulakis M. "Electron transfer-induced dehydrogenation reactions within methyl viologen-supported zeolite Na-Y under non-irradiative conditions" *Tetrahedron Lett*. **42**, (2001), 6409-6411.

[28] Sinfelt J. H., "Role of surface science in catalysis" *Surface Science* **500**, (2002), 923–946.

[29] Sheldon R. A., Bekkum H. (Eds) "Fine Chemicals through Heterogeneous Catalysis"2001(source:http://www.wileyeurope.com/WileyCDA/WileyTitle/productCd-35272995 13,descCd-description.html)

[30] Baiker A.; "Heterogeneous Catalysis: From Fundamentals to Reaction Engineering" *Chimia*, **50**, (1996), 65-73.

[31] Weitkamp, J.; Puppe, L.; (Eds); *Catalysis and Zeolites, Fundementals and Applications* (Springer-Verlag Berlin Heidelberg 1999), introduction

[32] Weitkamp, J.; "Zeolites and Catalysis" *Solid State Ionics*, **131**, (2000), 175-188.

[33] Coluccia S., Marchese L., Martra G.; "Characterisation of microporous and mesoporous materials by the adsorption of molecular probes: FTIR and UV–Vis studies" *Microporous and Mesoporous Materials*, **30**, (1999), 43–56.

[34] Corma A., García H.; "A unified approach to zeolites as acid catalysts and as supramolecular hosts exemplified" *J. Chem. Soc., Dalton Trans*. (2000), 1381–1394.

[35] Cano M. L., Coma A., Fornés V., Garcia H.; "Acid Zeolites as Electron Acceptors. Generation of Xanthylium, Dibenzotropylium, and Fluorenylium Cations from Their Corresponding Hydrides through an Electron-Transfer Mechanism" *J. Phys. Chem*. **99**, (1995), 4241-4246.

[36] Berkhout S.; "Intrazeolite Photophysics and Photochemistry", (Literature Study, University of Amsterdam, 1997).

[37] Coombs D. S., Alberti A., Armbruster T., Artoli G., Colella C., Galli E., Grice J. D., Liebau F., Mandarino J. A., Minato H., Nickel E. H., Passaglia E., Peacor D. R., Quartieri S., Rinaldi R., Ross M., Sheppard R. A., Tillmanns E., Vezzalini G.; "Recommended nomenclature for zeolite minerals: Report of the subcommittee on zeolites of the International Mineralogical Association, Commission on New Minerals and Mineral Names" (IMA Zeolite Report, 1998).

[38] Virta R. L.; "Zeolites" (source: http://minerals.usgs.gov/minerals/pubs/commodity /zeolites/ 2002).

[39] Breck, D.W., *Zeolites Molecular Sieves: Structure, Chemistry and Use*, (Wiley, NY, 1974), chapter one.

[40] Tosheva, L.; "Molecular Sieve Macrostructures Prepared by Resin Templating", (Doctoral Thesis, Lulea University of Technology, 2001).

[41] Hashimoto S.; "Zeolite photochemistry: impact of zeolites on photochemistry and feedback from photochemistry to zeolite science" *J. Photochem. Photobiol. C: Photochem. Rev. 4*, (2003), 19–49.

[42] Hashimoto S.; "Zeolites as single electron donors for photoinduced electron transfer reactions of guest aromatic species. Diffuse reflectance laser photolysis study" *J. Chem. Soc., Faraday Trans*. **93**, (1997), 4401-4408.

[43] Climent M. J., Corma A., Iborra S., Velty A.; "Designing the adequate base solid catalyst with Lewis or Bronsted basic sites or with acid–base pairs" *J. Mol. Catal. A: Chem.* **182–183**, (2002), 327–342.

[44] Ramamurthy V., Lakshminarasimhan P., Grey C. P., Johnston L. J.; "Energy transfer, proton transfer and electron transfer reactions within zeolites" *Chem Commun*. (1998), 2411–2424.

[45] Diddams P.; "Inorganic supports and catalysts – an overview" In: *Solid Supports and Catalysts in Organic Synthesis*, (Ed) K. Smith, Ellis (Horwood PTR Prentice Hall, 1992).

[46] Espeel, P.; Parton, R.;Toufar, H.;Martens, J.; Hölderich, W.;Jacobs, P.; "Zeolite Effects in Organic Catalysis" In: *Catalysis and Zeolites, Fundementals and Applications* ,(Eds) J. Weitkamp,; L Puppe, (Springer-Verlag, Berlin Heidelberg, 1999).

[47] Frei H., Blatter F., Sun H.; "Selective thermal and photooxidation of hydrocarbons in zeolites by oxygen" *United States Patent* 5 914 013 (22.06.1999)

[48] Kühl, G.H.; "Modification of Zeolites" In: *Catalysis and Zeolites, Fundementals and Applications*, (Eds) J. Weitkamp,; L Puppe, (Springer-Verlag, Berlin Heidelberg, 1999)

[49] Ichikawa M.; "Ship-in-Bottle Catalyst Technology. Novel Templating Fabrication of Platinum Group Metals Nanoparticles and Wires In Micro/Mesopores" *Platinum Metals Rev*. **44**, (2000), 3-14.

[50] Marriott P. J., Shellie R., Cornwell C.; "Gas chromatographic technologies for the analysis of essential oils" *J. Chromatogr. A*, **936**, (2001), 1–22.

[51] Wang T., Španěl P., Smith D.; "Selected ion flow tube, SIFT, studies of the reactions of H_3O^+, NO^+ and O_2^+ with eleven $C_{10}H_{16}$ monoterpenes" *Int. J. Mass Spectrom.* **228**, (2003), 117–126

[52] Augusto F., Lopes A. L., Zini C. A. "Sampling and sample preparation for analysis of aromas and fragrances" *Trends Anal. Chem*. **22**, (2003), 160-169.

[53] López C. M., Machado F. J., Rodríguez K., Méndez B., Hasegawa M., Pekerar S. "Selective liquid-phase transformation of a-pinene over dealuminated mordenites and Y-zeolites" *Appl. Catal. A: Gen*. **173**, (1998), 75-85.

[54] Kirk, Othmer, *Sulfur Encyclopedia of chemical technology*, 19, second edition, (John Wiley and Sons Inc, New York, 1969).

[55] Selvaraj M., Pandurangan A., Seshadri K.S., Sinha P.K., Krishnasamy V., Lal K.B.; "Comparison of mesoporous Al-MCM-41 molecular sieves in the production of p-cymene for isopropylation of toluene" *J. Mol. Catal. A: Chem.* **186**, (2002), 173–186.

[56] “Limonene Practical” (Source: http://www.chemsoc.org).

[57] Reggel L., Friedman S., Wender I.; “The Lithium-Ethylenediamine System. II. Isomerization of Olefins and Dehydrogenation of Cyclic Dienes” *J. Org. Chem*. **23**, (1958), 1136.

[58] Hoelderich W., Fischer R., Mross W. D., Pape F. F.; “Preparation of alkylbenzenes” United States Patent 4 665 252 (12.05.1987) BASF AG.

[59] Selvaraj M., Pandurangan A., Seshadri K.S., Sinha P.K., Lal K.B.; “Synthesis, characterization and catalytic application of MCM-41 mesoporous molecular sieves containing Zn and Al*” Appl. Catal. A: Gen*. **242**, (2003), 347–364.

[60] Stratakis, M.; Stavroulakis M., Sofikiti N.; “Thermal transformation of monoterpenes within thionin-supported zeolite NaY. Acid catalyzed or electron transfer induced?” *J. Phys. Org. Chem*. 16, (2003), 16–20.

[61] Lin H. P., Cheng S., Mou C. Y.; “Effect of delayed neutralization on the synthesis of mesoporous MCM-41 molecular sieves” *Microporous Materials*, **10**, (1997), 111-121.

[62] Scanning Electron Microscopy/X-Ray Diffraction Facility, (Source: http://www.earth.cf.ac.uk/asg/sem_xrd.html)

[63] Varma R. S.; “Clay and clay supported reagents in organic synthesis”, *Tetrahedron*, **58**, (2002), 1235-1255.

[64] Shichi T., Takagi K.; “Clay minerals as photochemical reaction fields” *J. Photochem. Photobiol. C: Photochem. Rev. 1* (2000), 113–130.

[65] X. Liu, Iu K. K., Thomas J. K., He H., Klinowski J.; “Spectroscopic Studies of Protonated Aromatic Species and Radical Cations in H^+-Zeolites” *J. Am. Chem. Soc*. **116**, (1994), 11811-11818.

[66] Hunter G.L., Brogden W.B.; "Isomerization and Disproportionation of &Limonene on Silica Gel" *J. Org. Chem*. **28**, (1963), 1679.

[67] Gutjahr M., Pöppl A., Böhlmann W., Boöttcher R.; "Electron pair acceptor properties of alkali cations in zeolite Y: an electron spin resonance study of adsorbed di-tert-butyl nitroxide" *Colloids and Surfaces A: Physicochem. Eng. Aspects*, **189**, (2001), 93–101.

[68] Zhou, W.; Clennan, E. L.; "Spontaneous oxidation of a sulfide in zeolite CaY: the unprecedented reaction of a sulfide radical cation with oxygen" *J. Chem. Soc., Chem. Commun*. (1999), 2261–2262.

[69] Lakshminarasimhan P., Thomas K. J., Brancaleon L., Wood P. D., Johnston L. J., Ramamurthy V.; "Characterization of Persistent Intermediates Generated upon Inclusion of 1,1-Diarylethylenes within CaY Zeolite: Spectroscopy and Product Studies" *J. Phys. Chem. B*, **103***,* (1999), 9247-9254.